PHYTOPLANKTON ECOLOGY
IN A
HIGH ARCTIC POLYNYA

BY

JOANNE ELIZABETH BUTLER

B.Sc., The University of Alberta, 1979

A THESIS SUBMITTED IN PARTIAL FULFILLMENT OF

THE REQUIREMENTS FOR THE DEGREE OF

MASTER OF APPLIED SCIENCE

in

THE FACULTY OF GRADUATE STUDIES

(Civil Engineering Dept., Environmental Engineering Group)

We accept this thesis as conforming

to the required standard

2'4

THE UNIVERSITY OF BRITISH COLUMBIA

March 1985

In presenting this thesis in partial fulfilment of the requirements for an advanced degree at the University of British Columbia, I agree that the Library shall make it freely available for reference and study. I further agree that permission for extensive copying of this thesis for scholarly purposes may be granted by the head of my department or by his or her representatives. It is understood that copying or publication of this thesis for financial gain shall not be allowed without my written permission.

Department of Civil Engineering

The University of British Columbia
2075 Wesbrook Place
Vancouver, Canada
V6T 1W5

Date 15 March 1985

ABSTRACT

Primary production was studied in Fram Sound, part of the Hell Gate-Cardigan Strait polynya, from June to August, 1982. Primary production rates, phytoplankton biomass (chlorophyll a), and water transparency were measured and used in conjunction with modelled solar radiation values to numerically model primary production during this time. The major phytoplankton nutrients were also measured.

Early season chlorophyll a concentrations were low, and the increased light availability due to reduced ice cover in this area did not appear to enhance early season production. Chlorophyll concentrations peaked twice; the first peak occured on 20 July and the second on 14 August. The mean primary production rate and phytoplankton biomass were 998 mg $C.m^{-2}.d^{-1}$ and 72 mg $chl.m^{-2}$. This production rate is higher than that measured in other High Arctic areas.

Nitrogen, phosphorus and silica were essentially homogeneously distributed during the sampling period and these concentrations varied little from June to August except during 5 days in late August, when they decreased by half then returned to previous levels.

Supervisors: _____

TABLE OF CONTENTS

LIST OF FIGURES

LIST OF TABLES

ACKNOWLEDGEMENTS

My sincere thanks to all the people who have helped tranform my desire to learn about the Arctic from a project idea into the reality of a finished thesis.

The Environmental Engineering Group of the Civil Engineering Department at the University of British Columbia (UBC) gave me a place to start. Financial support was initially provided by the National Science and Engineering Research Council and later by a UBC Graduate Fellowship. Prof. Jim Atwater and Dr. Bill Oldham of this Department allowed me the opportunity to pursue a project of my choice. Jim Atwater's support and flexibility as my supervisor at UBC enhanced all phases of my learning process in this program.

Dr. Buster Welch of the Freshwater Institute, Winnipeg, agreed to supervise and financially support my project while I was still at UBC, gave me the freedom to learn on my own, and many times helped me find the path when I was lost in the woods. I have benefited greatly from his willingly shared enthusiasm and knowledge of the Arctic and science.

Gerry Prach and Al Smith of the Canadian Wildlife Service (CWS) provided some logistic support at Cape Vera during the 1982 field season. Many thanks to Tim Siferd, who provided support and invaluable assisstance in the field and to Alex Dzubin (CWS) for his encouragement at Cape Vera. The Polar Continental Shelf Project (Resolute Bay), headed by George Hobson, of the Department of Energy, Mines and Resources (EMR) generously supplied logistic support and generators.

The helpful suggestions and solar radiation literature given by Dr. Bea Alt (EMR Ottawa) were greatly appreciated.

To the many gifted and kind people at the Freshwater Institute, Winnipeg, who have helped during the data analysis and writing phases of this thesis I offer my heartfelt thanks. Particular thanks to Dr. Everett Fee, who provided the numerical model I used to calculate primary production and who graciously answered countless software questions; to John Legault, who expedited the equipment for my field work and helped in many ways; and to Ron Lypka, who gave computer advice and helped with the solar radiation model program. Mike Stainton and the Analytical Chemistry Section analysed the nitrogen and phosphorus nutrient samples, Hedy Kling identified phytoplankton samples, Eric Marshall and the Library staff readily accessed even the most obscure literature, and Andries Blouw and the Graphics Dept. willingly and skillfully transformed rough maps and diagrams into informative figures. Dr. Jim Reist provided statistical advice and Kathleen Martin-Bergmann made several helpful suggestions on earlier drafts of this manuscript. Martin Bergmann also gave many helpful suggestions along the way. I am grateful to Gordon Koshinsky and Buster Welch for providing the opportunity for uninterrupted writing last summer.

For the moral support, encouragement and patience of Rob Walker during the data analysis and writing stages of this thesis I can only say thank-you very much and it's finished!

INTRODUCTION

> Otto Sverdrup described his first view of the open water of Hell Gate (March 1900) as an area where " great pressure hummocks were drifting along at terrific speed in the violent whirlpool caused by the strong tidal current", and that "none of us had ever seen waters so utterly impossible to navigate as the sound here" (in Taylor 1955).

Polynyas are areas of water, surrounded by sea ice, where ice cover is reduced or absent for all or most of the year. Annually occuring polynyas found in the same location are called recurring polynyas and are distributed throughout the Canadian Arctic (Fig. 1). They range in size from the Cambridge Fiord polynya, south of Pond Inlet, with a surface area of less than 1 km^2, to the North Water, estimated to be 100,000 km^2 (Dunbar 1981).

These areas of open water are formed and maintained by various combinations of wind, strong set (permanent) currents, tidal currents and upwellings of warmer deep water, and Dunbar (1981) has comprehensively reviewed several theories on the interaction of these factors. Wind is the most important factor in the formation and maintenance of polynyas.

Figure 1. Map of the recurring polynyas in the Canadian Arctic (from Smith and Rigby 1981).

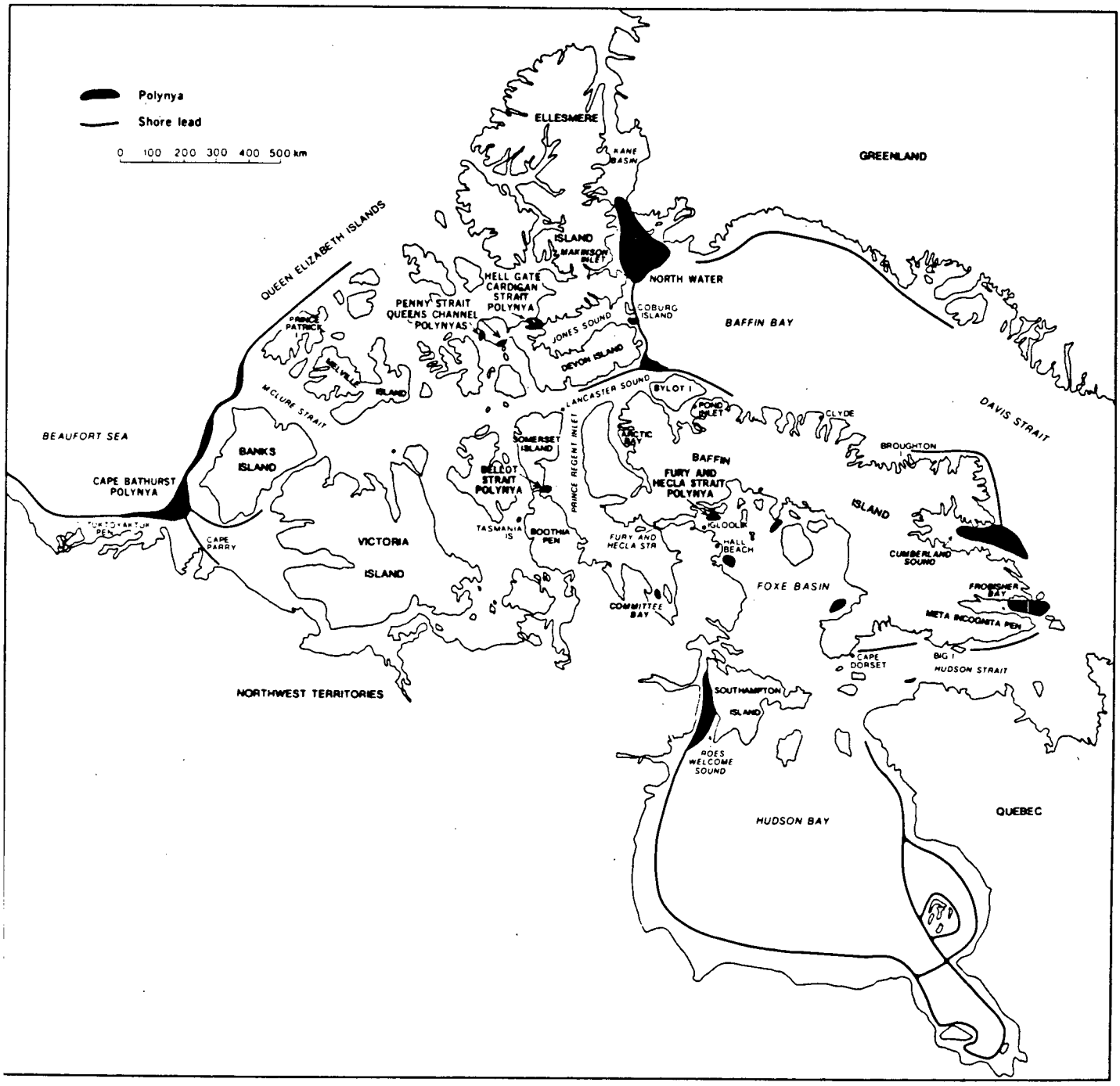
Polynya
Shore lead
0 100 200 300 400 500 km
ELLESMERE
ISLAND
KANE BASIN
MARKHAM INLET
GREENLAND
NORTH WATER
BAFFIN BAY
QUEEN ELIZABETH ISLANDS
HELL GATE
CARDIGAN STRAIT POLYNYA
PENNY STRAIT
QUEENS CHANNEL POLYNYAS
PRINCE PATRICK ISLAND
MELVILLE ISLAND
JONES SOUND
COBURG ISLAND
DEVON ISLAND
LANCASTER SOUND
BYLOT I.
POND INLET
CLYDE
DAVIS STRAIT
M'CLURE STRAIT
BEAUFORT SEA
BANKS ISLAND
SOMERSET ISLAND
ARCTIC BAY
BROUGHTON ISLAND
CAPE BATHURST POLYNYA
BELLOT STRAIT POLYNYA
PRINCE REGENT INLET
BAFFIN
FURY AND HECLA STRAIT POLYNYA
TUKTOYAKTUK PEN.
CAPE PARRY
TASMANIA IS.
BOOTHIA PEN.
FURY AND HECLA STR.
GLOOSCAP
HALL BEACH
CUMBERLAND SOUND
VICTORIA ISLAND
FOXE BASIN
FROBISHER BAY
COMMITTEE BAY
META INCOGNITA PEN.
CAPE DORSET
BIG I.
HUDSON STRAIT
NORTHWEST TERRITORIES
SOUTHAMPTON ISLAND
ROES WELCOME SOUND
HUDSON BAY
QUEBEC

Offshore winds remove newly formed ice from the lee shores and induce upwellings. The formation of sea ice increases the salinity of the surrounding water by freezing out solutes. When new ice is continually formed (which occurs in areas with strong prevailing winds) the salinity of surface water increases until it is denser than the water below, and subsequently sinks. When the deep water is warmer than the surface water, this sinking, called haline convection, results in a vertical exchange of water by displacement and heat is brought to the surface. The North Water, Cape Bathurst polynya and the Baffin Island coastal flaw lead have underlying layers of warmer water. It is postulated that these areas are formed and maintained by this combination of strong prevailing winds, haline convection and warm deep water (Dunbar 1981).

Ice can also be mechanically removed by strong tidal currents. Dunbar (1981) suggests that this mechanism is probably the most dominant force maintaining the polynyas in Cumberland Sound and Frobisher Bay, where the tidal ranges reach 7.6 m and 13.1 m respectively (Sailing Directions-Arctic Canada 1982). A combination of set and tidal currents help maintain the Hell Gate-Cardigan Strait, Penny Strait and Queens Channel polynyas (Smith and Rigby 1981).

The biological importance of polynyas is attested to by the large number of marine birds and mammals associated with them, although few quantitative studies have been conducted to investigate their ecological significance (Stirling 1981). The Cape Bathurst polynya in the Beaufort Sea serves as a spring staging area for migrating beluga (Delphinapterus leucas) and seabirds, as an overwintering area for subadult ringed seals

(Phoca hispida) and bearded seals (Erignathus barbatus). Lancaster Sound is a major feeding and breeding area for 2 to 3 million marine birds and approximately 40,000 beluga and narwal (Monodon monoceros) annually, many of which congregate in the area between Devon and Bylot Islands from early spring to late autumn (Milne and Smiley 1978). The Fram Sound area supports a large colony (~10,000 pairs) of Northern Fulmars (Fulmaris glacialis) which nest near Cape Vera at the south end of the polynya from early May to late September, and the morthernmost known colony of Common Eiders (Somateria mollissima borealis) which nest on St. Helenas Island in Fram Sound (Prach et al. unpub. data). Walrus (Odobenus rosemarus), ringed seal, bearded seal and polar bear (Ursus maritimus) were frequently seen during aerial surveys of the Hell Gate-Cardigan Strait polynya (pers.obs.). Approximately 100 walrus overwinter in the Penny Strait area each year (Stirling pers. comm.).

A combination of factors probably accounts for the supposed high biological productivity associated with polynyas and nearby areas; the presence of open water for most or all of the year increases opportunities for marine birds and mammals to feed, and the fact that wildlife congregates in such areas suggests that food is indeed available. Offshore oil and gas production and the imminent need for year-round shipping threaten to disturb several polynyas, since the absence of sea-ice for all or most of the year make these areas attractive shipping corridors. The Cape Bathurst polynya and Lancaster Sound are on the proposed tanker route for the year-round transportation of oil and gas to southern markets (Beaufort Sea Hydrocarbon Production and Transportation Proposal 1984).

Hell Gate-Cardigan Strait and Fram Sound, a recurring polynya in the Canadian High Arctic, is the site of a long term ecological study begun by the Canadian Wildlife Service (CWS, Edmonton) in 1980 to provide baseline data on the biological significance of this area to marine wildlife. The purpose of the current study was to measure primary productivity at Fram Sound and incorporate these data into the CWS database. The contribution of early season production in Arctic polynyas has not previously been studied; the effects of reduced ice cover with the onset of polar day suggests primary production may proceed earlier than in surrounding ice-covered areas.

The base of the marine food chain is mainly phytoplankton, single-celled photosynthetic organisms which synthesize organic carbon from carbon dioxide (CO_2) and water in the presence of light. This is refered to as primary production, and the rate of primary production, called primary productivity, is indicative of the production of higher trophic levels (Parsons et al. 1979).

Primary productivity is commonly measured with a radioactive (^{14}C) bioassay. A known concentration or activity of radioactive carbon is added to several water samples, and each sample is incubated at one of a series of light levels for a known time (Steeman-Nielsen 1952). Chlorophyll a, a photosynthetic pigment extracted from concentrated phytoplankton, is used as an index of phytoplankton biomass, and ^{14}C-uptake rates are generally normalized to chlorophyll a. The amount of ^{14}C taken up by the phytoplankton is used to determine a light response at various light levels, and these measurements are in turn used to estimate the rate of primary production as a function of light

in the sea.

The quality and quantity of solar radiation change as the light penetrates the water column. The longer wavelengths are attenuated near the surface, usually within the top 10 m. The quantity of photosynthetically active radiation (PAR, 400-700 nm waveband) decreases exponentially with depth and strongly affects the rate of primary production. Measurements of submarine light, chlorophyll a concentrations and ^{14}C-uptake at various depths over time provide the necessary information to model primary productivity for the area being studied.

Nitrogen, phosphorus and silica are phytoplankton nutrients, and their concentrations are often measured in conjunction with primary productivity studies to reveal if nutrients, particularly nitrate or silica in the sea, may be limiting productivity rather than light. Concentrations of these essential nutrients frequently change seasonally and with depth, depending on local and large scale hydrological conditions.

Specific objectives of this study were: 1) to measure primary productivity (using ^{14}C), chlorophyll a concentrations, water transparency and incoming solar radiation from June to August, 1982, 2) to model primary productivity in the Fram Sound area using the numerical method of Fee (1984), and 3) to measure the spatial and temporal distribution of nutrients. These data will then be incorporated in the CWS Hell Gate-Cardigan Strait Polynya Project database.

MATERIALS AND METHODS

Study Area

Hell Gate and Cardigan Strait are narrow channels through which water from Norwegian Bay flows into Fram Sound before entering the west end of Jones Sound. These two channels and Fram Sound form the Hell Gate-Cardigan Strait polynya, located approximately between 76°20'-76°50'N latitude and 89°30'-90°00'W longitude (Fig. 2). This polynya is maintained by a combination of strong set and tidal currents (Smith and Rigby 1981). The set or permanent current, which flows south from Norwegian Bay, ranges from 1.5 to 3.5 knots (Pilot of Arctic Canada 1978). Strong winds at Cape Vera up to 70 knots (pers. obs.) probably influence the extent of ice formation and the movement of ice in Fram Sound.

The maximum extent of open water in the polynya occurs in May, June and July. In September the bays and fiords freeze with new ice, and in October and November the straits are clogged with older ice from Norwegian Bay (Smith and Rigby 1981). Open water is generally present in early December, and from then until spring the extent of open water varies (Fig. 3).

Fram Sound was the area sampled for the present study. The depth of Fram Sound ranges from 150-200 meters mid-channel to a shallow water

Figure 2. Locator map of the study area. Norwegian Bay flows into Jones Sound through Hell Gate, Cardigan Strait and Fram Sound. Cape Vera was the base camp for the present study.

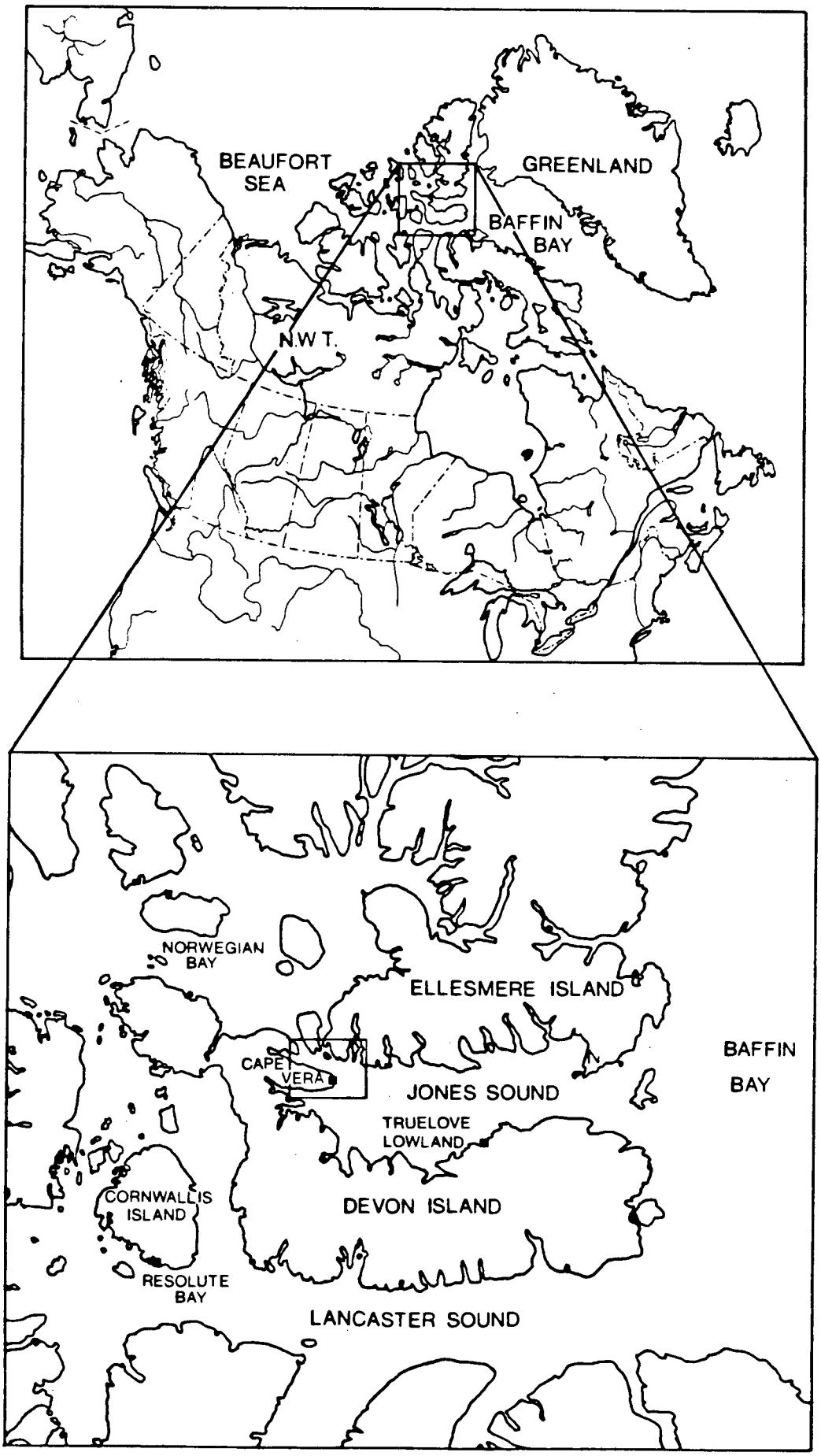
BEAUFORT SEA
GREENLAND
BAFFIN BAY
N.W.T.
NORWEGIAN BAY
ELLESMERE ISLAND
BAFFIN BAY
CAPE VERA
JONES SOUND
TRUELOVE LOWLAND
CORNWALLIS ISLAND
DEVON ISLAND
RESOLUTE BAY
LANCASTER SOUND

Figure 3. Map of ice conditions in the Hell Gate-Cardigan Strait polynya. (from Smith and Rigby 1981).

large black areas indicate open water to 1/10 ice cover
thin line leading into thicker line indicates a crack/lead
single thin line indicates division between ice cover categories
L indicates an open lead and is inserted in some cases where the lead is not obvious

1 2/10 – 5/10 ice cover
2 6/10 – 7/10 ice cover
2+ 8/10 ice cover
3 9/10 – 10/10 ice cover

F fast ice
N new ice
O old ice
M multiyear ice
A 1st-year ice
< A less than 1st-year ice

S 2nd-year ice
U unknown
G grey ice
W grey-white ice

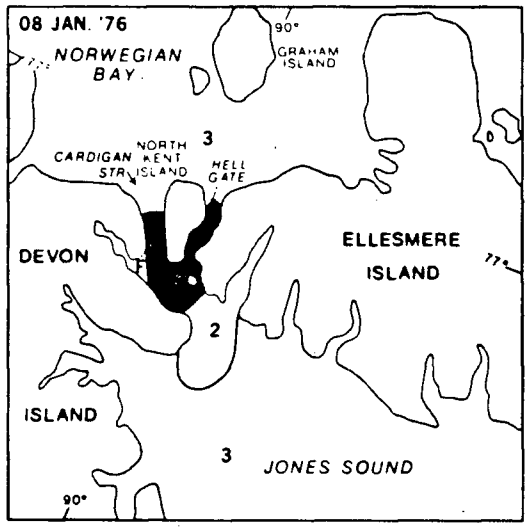

a

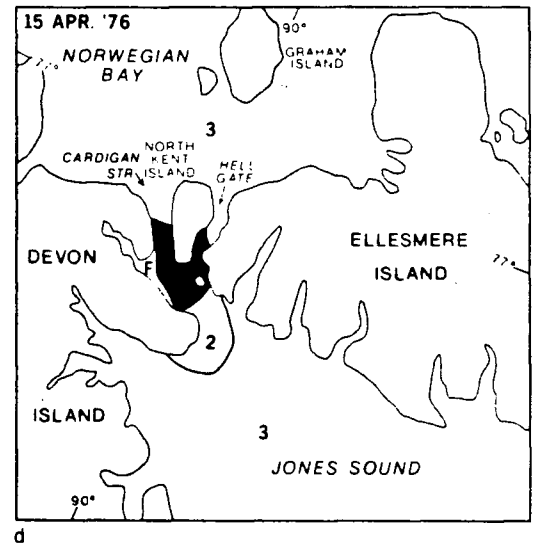

d

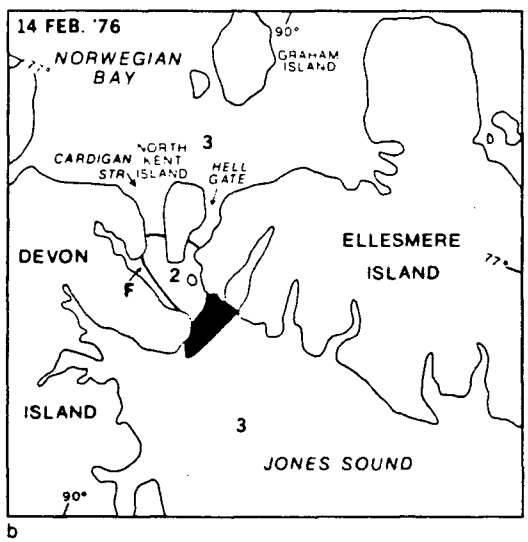

b

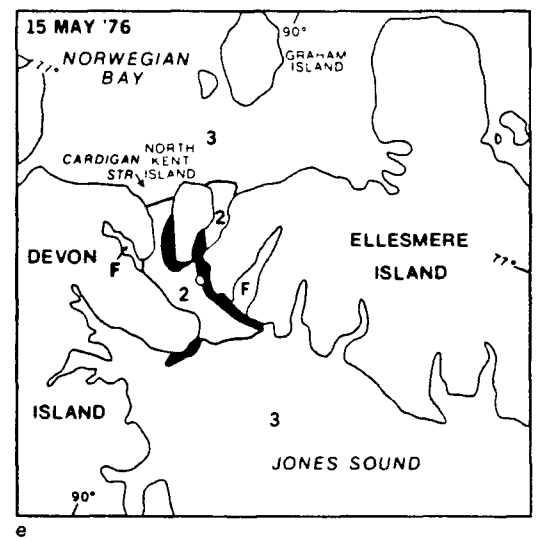

e

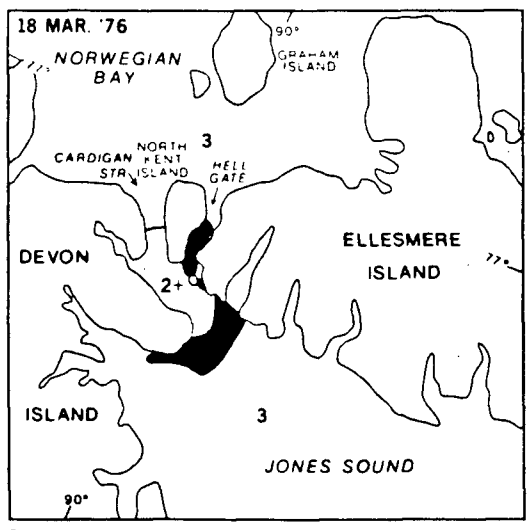

c

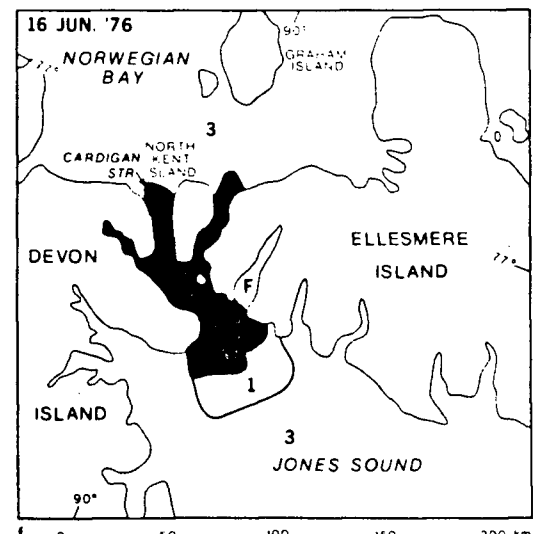

f

0 50 100 150 200 km

margin (about 1 km) of less than 50 meters along the southwestern shore. This shallow zone extends to approximately 5 km off the tip of Cape Vera. Tides in this area are semidiurnal; at the Bay of Woe the maximum and average tidal ranges are 3 m and 1.3 m respectively (P. Davies, Canadian Hydrographic Service, pers. comm.).

Sampling

Fram Sound was sampled from 30 May to 17 August 1982. Sampling locations varied as necessitated by ice and weather conditions; strong winds and moving pack ice often restricted sampling to nearshore locations (Fig 4). When conditions permitted, more than one location was sampled on the same day to test for homogeneity of the water mass. Two locations were sampled on July 5 (Locations E,F) July 20 (L,M), August 2 (R,S), August 5 (T,U) and August 16 (X,Y). Three locations were sampled on August 17 (Z,AA,BB).

An opaque polyvinylchloride (PVC) 2 L Van Dorn bottle was used to collect discrete samples, which were usually taken from 0,2,5,10,and 20 m. At locations where the maximum depth exceeded 20 m and weather conditions permitted, sampling was extended to 30,40,50 and 75 m. Samples were transferred to opaque 2 L polyethylene Nalgene bottles in the shade to avoid light shock, and kept cold and dark until analysed.

Samples were usually processed within 2 h of collection. Subsamples were analysed in the field laboratory for chlorophyll a and silica concentrations; dissolved and suspended nutrients subsamples were preserved for later analysis at the Freshwater Institute (FWI). Radioactive carbon (^{14}C) uptake experiments were conducted in the field

Figure 4. Map of the locations sampled in Fram Sound from 30 May to 17 August, 1982. Sampling was often restricted to nearshore locations because of high winds and moving pack ice.

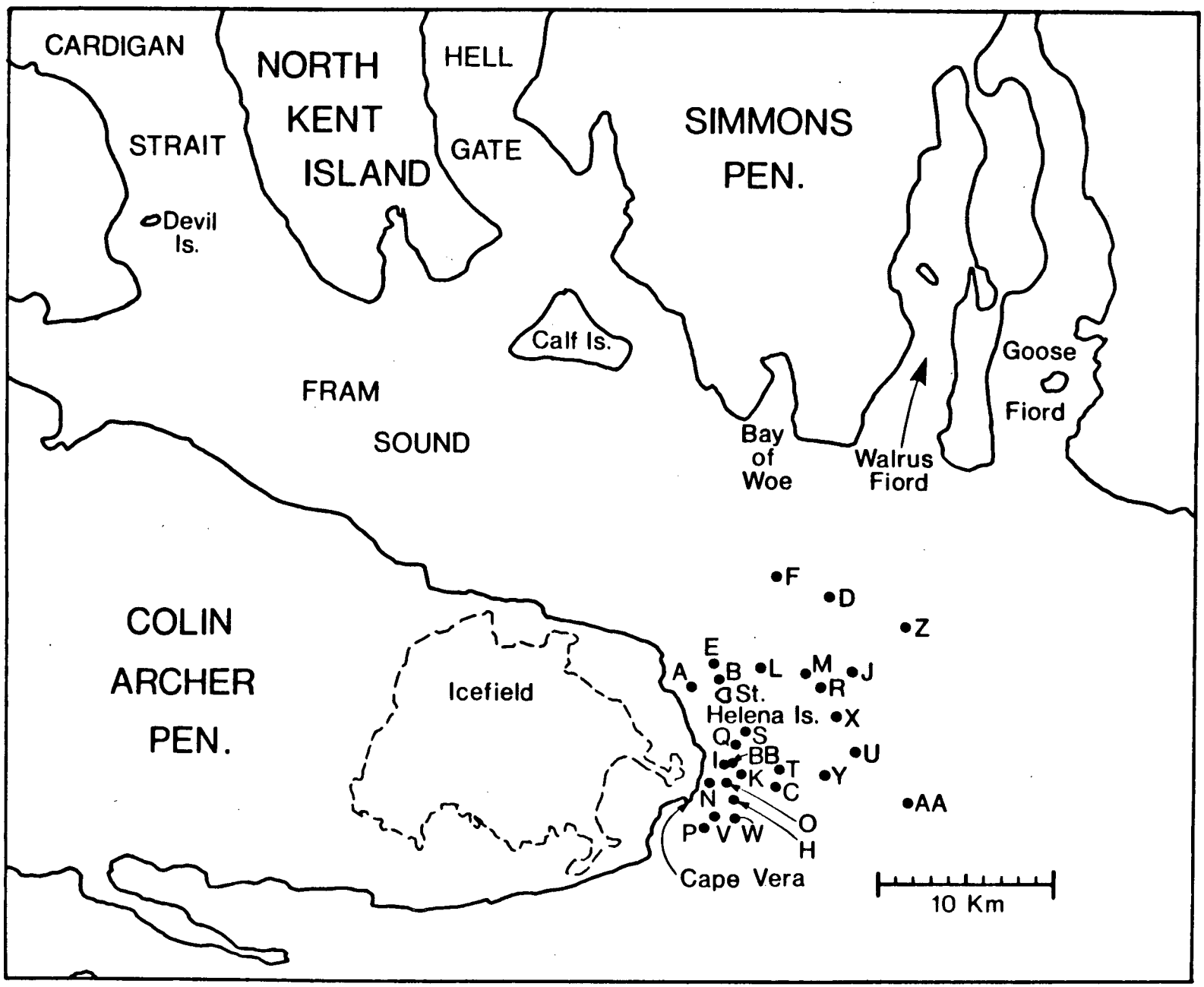
CARDIGAN
STRAIT
NORTH
KENT
ISLAND
HELL
GATE
SIMMONS
PEN.
Devil
Is.
Calf Is.
FRAM
SOUND
Bay
of
Woe
Walrus
Fiord
Goose
Fiord
COLIN
ARCHER
PEN.
Icefield
F
D
Z
E
A
B
L
M
J
St.
R
Helena Is.
X
Q
S
I
BB
U
T
Y
K
C
N
AA
O
P
V
W
H
Cape Vera
10 Km

lab and the concentration of ^{14}C was measured in Winnipeg.

Chlorophyll a

One hundred and seventy-two samples were analysed for phytoplankton chlorophyll a concentrations. Aliquots were vacuum filtered on Whatman GF/C glass fiber filters (4.25 cm) at 8 psi until almost dry. The filters were folded and chlorophyll a statically extracted with 10 ml of 99.5% acetone for approximately 24 h in the dark at 0-5^{o}C. Chlorophyll was measured fluorometrically using a Turner Model III fluorometer, calibrated according to the spectrophotometric method of Stainton et al.(1977). Chlorophyll is usually extracted in 90% acetone; to determine whether there was a quantitative difference in the chlorophyll concentrations extracted by these two concentrations of acetone, experimental extractions were done. These experimental extractions did not show a significant difference in the extraction efficiencies of these two concentrations of acetone (one-way analysis of variance, $p<0.05$).

Volumes filtered were 5-6 l at each depth on 30 May and 14 June, 2.5 l on 14 June and 2 July, and 0.5 l for the remaining sampling period. Subsamples (125 ml) were preserved with Lugol's solution and 10 % formalin for microscopic analysis on 2, 12 and 28 July and 2, 14 and 17 August.

Nutrient Chemistry

Silica

Soluble reactive silicon was measured in the field laboratory according to the manual colorimetric technique of Stainton et al. (1977). Duplicate measurements were made and the mean value reported.

Nitrogen and Phosphorus

Particulate nutrients (N,P) were collected on preignited (500°C for 16 h) Whatman GF/C filters, and the same volume was filtered for these samples as was used for chlorophyll determinations at each location. Particulate nitrogen samples were vacuum filtered to dryness, placed in plastic petri dishes and dessicated in the dark with a silica gel dessicant. Samples were analysed at the FWI by an automated combustion technique (Stainton et al. 1977). Particulate phosphorus samples were also filtered to dryness. The filters were placed in 20 ml Pyrex screw cap vials previously rinsed with filtrate, and later analysed at the FWI by the method of Stainton et al. (1977).

The filtrate from the particulate phosphorus filtration was retained for dissolved macronutrient analysis. Total dissolved nitrogen (TDN) and phosphorus (TDP) samples were preserved with 100 ul of 4N Ultrex sulphuric acid and later analysed according to an automated photocombustion technique (Stainton et al. 1977).

Physical Oceanography

At each location, submarine light (Photosynthetically Active Radiation,PAR) was measured using a LICOR LI-185A quantum meter with a Lambda flat-plate cosine-corrected quantum sensor. Surface light (in air) was recorded, and measurements were made at 1 m intervals to 27 m.

These water transparency measurements, recorded under constant sky conditions whenever possible, were taken to provide data for the calculation of the extinction coefficient (k). Light is attenuated exponentially with depth in the sea, and the intensity at any depth can be calculated from the following equation (Raymont 1980) when the extinction (or attenuation) coefficient is known:

$$I_d = I_o e^{-kd}$$

where I_d=light intensity at depth d

I_o=surface light intensity

k=extinction coefficient

d=depth

These data are then used to calculate the light intensity at different depths by a numerical primary production model (Fee 1984).

Water temperature was recorded to the nearest 0.1^oC using a bead thermistor probe and digital multimeter at 1m intervals.

Conductivity samples were heated to 25^oC in a water bath and conductivity measured using a Radiometer conductivity meter. Thirty samples were retained to determine salinity with an Autosal Laboratory Salinometer Model 8400, using UNESCO International Oceanographic tables. Salinity was linearly regressed with conductivity and the regression equation (sal=0.79*cond-6.81, r^2=0.97) was used to calculate salinity values from conductivity measurements.

Temperature and salinity data were used to calculate density according to the revised SCOR/UNESCO equations (International Oceanographic Tables 1972).

Primary Production

Photosynthesis-Light experiments

Microalgal photosynthetic rates were measured with ^{14}C-uptake in a shore-based incubator. The laboratory was darkened for the duration of the sample preparation and incubation period. This reduced light-shock to the samples during preparation and minimized stray light entering the incubator.

The samples were held in a water bath at in-situ temperatures (-1^{o}C) prior to preparation for incubation, and were inverted several times to thoroughly mix the contents before being poured into the reagent bottles. Four depths from the sampling profile, usually 2, 5, 10, and 20 m, were used for the photosynthesis-light experiments. Six pairs of 60 ml glass reagent bottles were filled to overflowing with water from each depth and then injected with 0.5 ml stock solution of 30 uC/ml $NaH^{14}CO_3$ in sterile saline. Five pairs of bottles were placed in each of five compartments in an incubator (Figs. 5,6 ;described in detail by Shearer et al. 1985); the sixth pair was darkened with aluminum foil as controls. The samples were incubated for 4 h in circulating seawater maintained at -1^{o}C. A 400 Watt Sylvania metalarc lamp illuminated the incubator; this light source closely approximated clear sky wavelengths in the PAR waveband (McCree 1972). Light levels in the incubator compartments were measured with the same quantum meter and sensor used for submarine light measurements. These incubator

Figure 5. Schematic diagram of the incubator used to measure the rate of primary production. Photosynthetically active radiation was measured in the incubator with a flat plate cosine-corrected sensor prior to and after the 4 h incubation, and later corrected for the backscattering of light in the incubator. (modified from Shearer et al. 1985).

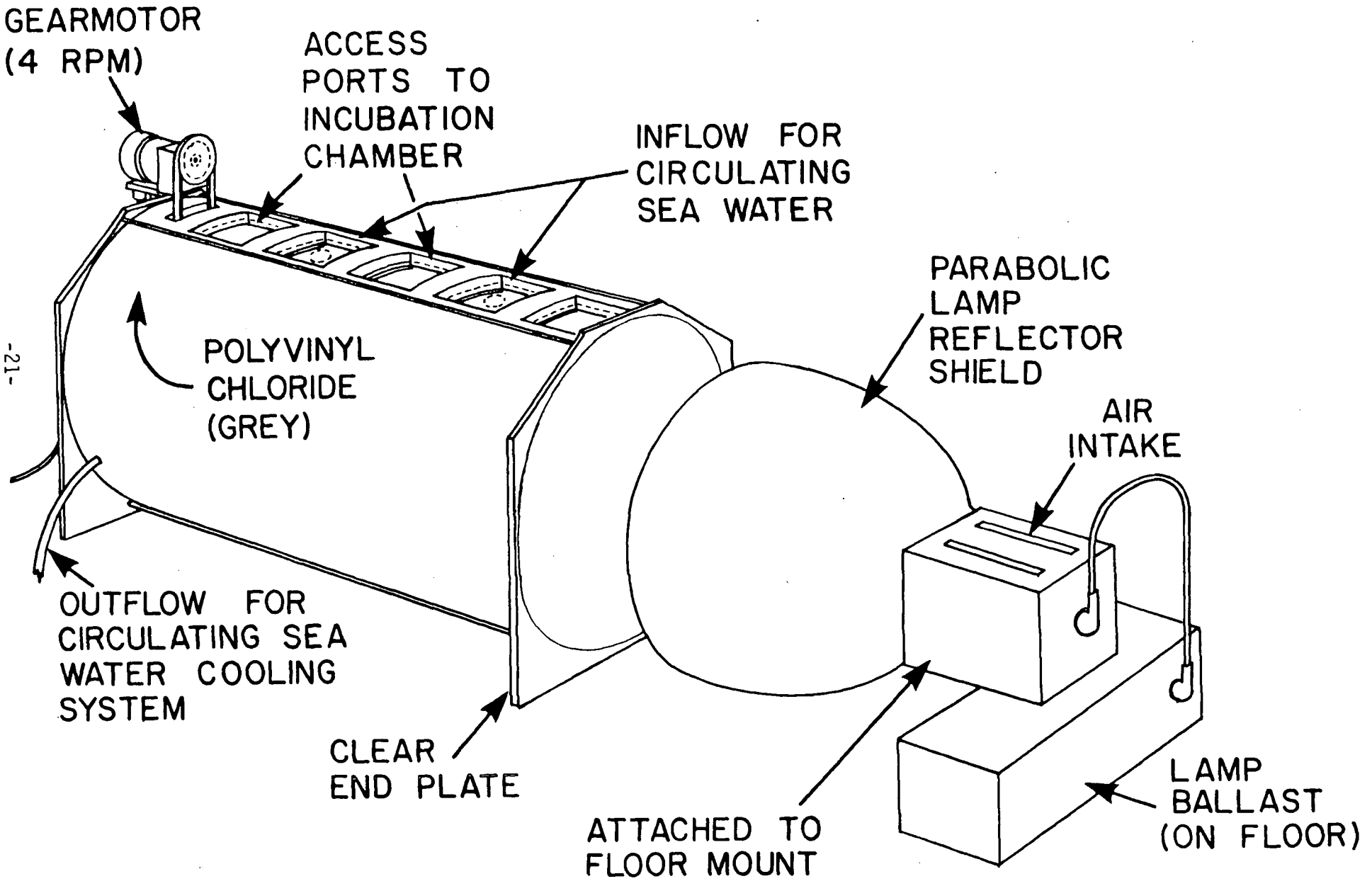
GEARMOTOR
(4 RPM)
ACCESS
PORTS TO
INCUBATION
CHAMBER
INFLOW FOR
CIRCULATING
SEA WATER
PARABOLIC
LAMP
REFLECTOR
SHIELD
POLYVINYL
CHLORIDE
(GREY)
AIR
INTAKE
OUTFLOW FOR
CIRCULATING SEA
WATER COOLING
SYSTEM
CLEAR
END PLATE
ATTACHED TO
FLOOR MOUNT
LAMP
BALLAST
(ON FLOOR)

Figure 6. Longitudinal and cross-sectional schematic diagram of the incubator used to measure the rate of primary production. Mounted samples rotated on plexiglass disks to mix the samples during the incubation. (modified from Shearer et al. 1985)

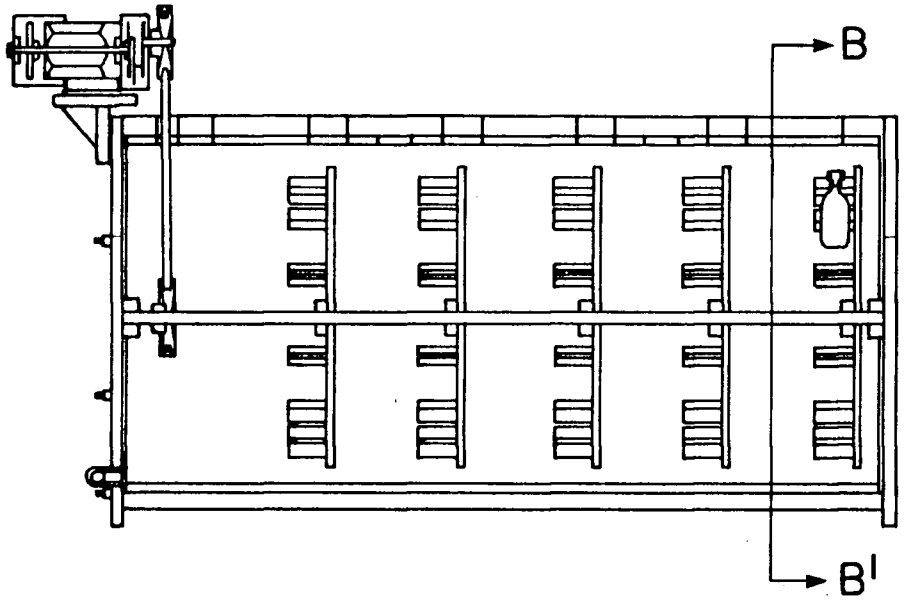

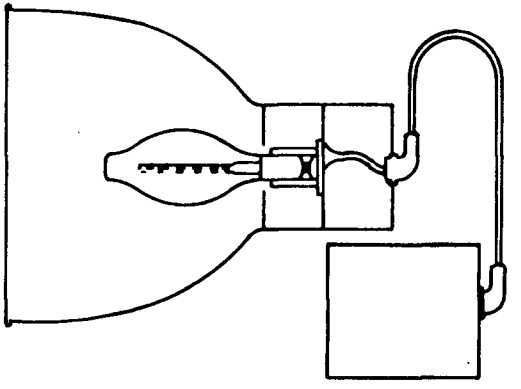

LONGITUDINAL SECTION A-A'

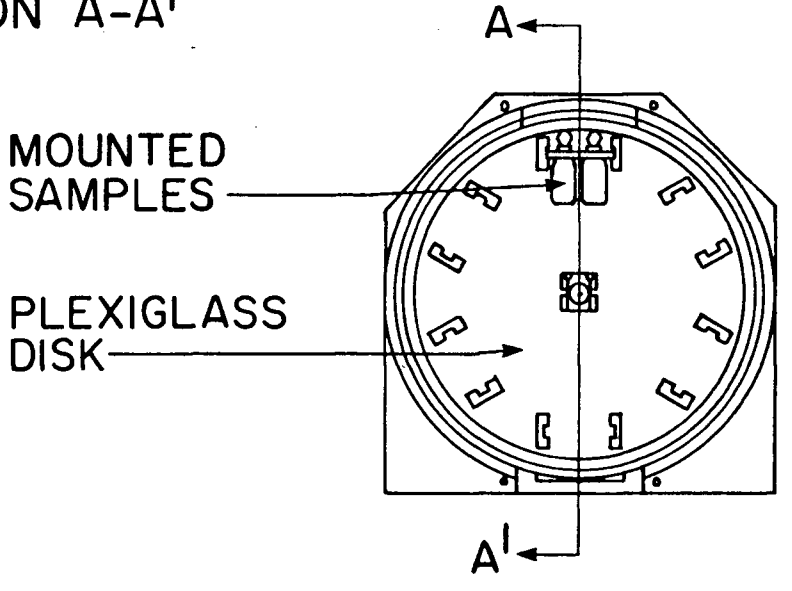

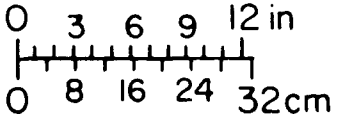

SCALE

CROSS SECTION B-B'

measurements were multiplied by empirical correction factors (1.84, 1.75, 1.66, 1.61, 1.60 from highest to lowest light chambers) to correct for the backscattering of light in the incubator (Shearer et al. 1985).

After incubation, radioactive carbon uptake was assayed on 8 ml aliquots placed in 20 ml scintillation vials by the acidification and bubbling method (Schindler et al. 1972). After the bubbling procedure 0.1 ml of NCS, a tissue solubilizer, was added to each sample with 10 ml of Beckman Ready-Solv MP fluor. Samples were counted with a Beckman LS 7500 liquid scintillation counter at the Freshwater Institute.

Alpha and P^B_m

The incubator data, which consisted of the photosynthetic response of the algae at 5 light levels, were used to calculate two parameters for each Photosynthesis-Irradiance curve; alpha, the slope of light-limited photosynthesis, and P^B_m, the rate of primary production at light saturation, both normalized to chlorophyll (Fig. 7). These calculations were done with a non-linear curve fitting technique developed by Fee (1984), using a modified version of the hyperbolic tangent function recommended by Jassby and Platt (1976). From these values, the mean alpha and P^B_m were calculated and subsequently used in a computer program which models primary production (Fee 1984).

Primary Production Model

To simulate primary production, this numerical model requires alpha and P^B_m values, water transparency and chlorophyll measurements, and solar radiation data. Production was calculated at intervals of 30

Figure 7. A Photosynthesis-Irradiance curve, showing alpha, the slope of light-limited photosynthesis, I_k, the irradiance at the onset of light saturation, and $P^B m$, the rate of primary production at light saturation. Alpha and $P^B m$ were simultaneously determined with a non-linear least squares computer program developed by Fee (1984).

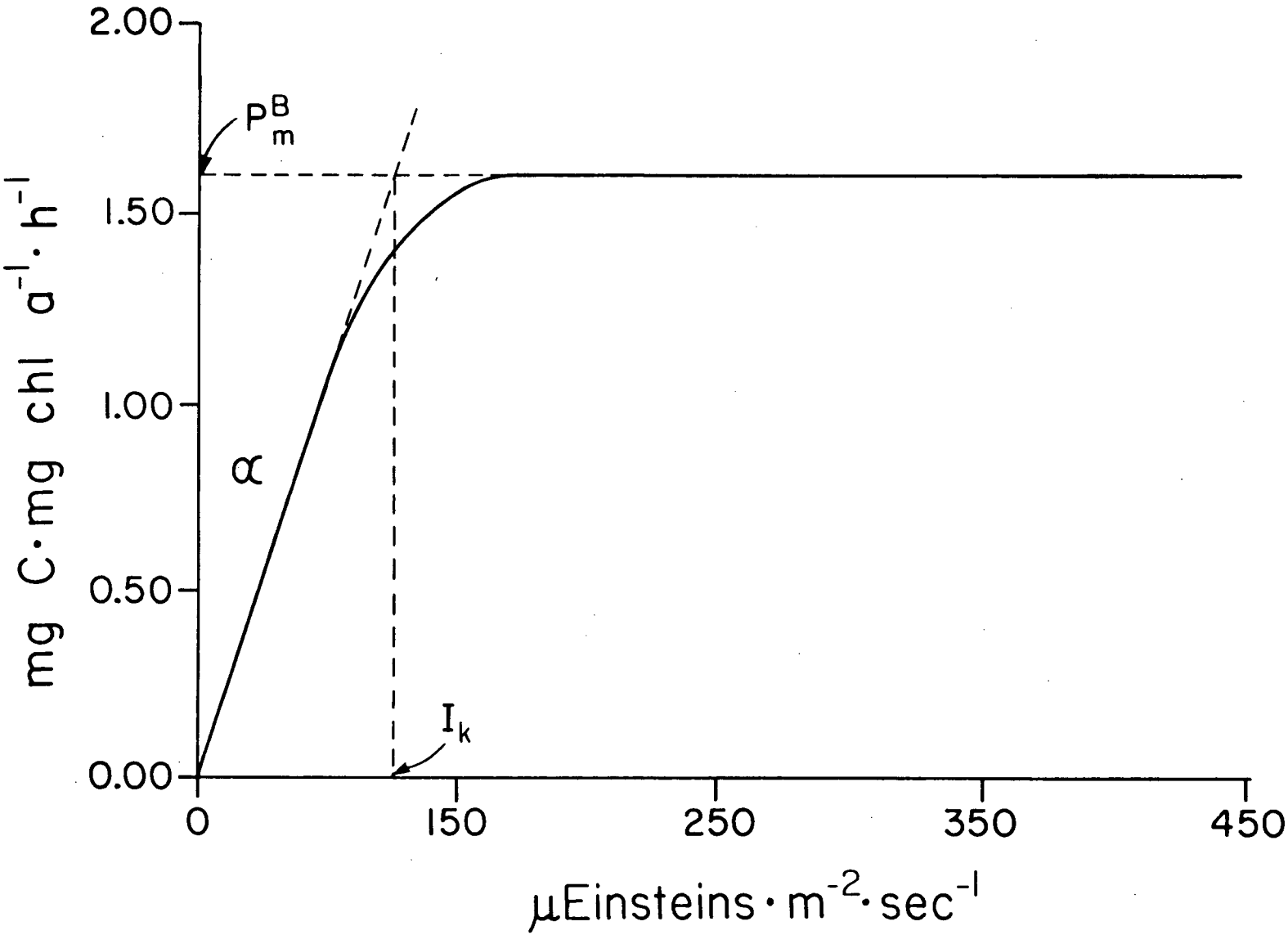
2.00
1.50
1.00
0.50
0.00
P^B_m
α
I_k
0
150
250
350
450
mg C · mg chl $a^{-1} \cdot h^{-1}$
μEinsteins · $m^{-2} \cdot sec^{-1}$

minutes at 11 depths for each day. The absolute light value at each depth was calculated from solar radiation data and water transparency profiles, and used to calculate primary production from alpha and $P^B m$ values according to the following equations from Fee (1984):

$$P^B = 0 \qquad \text{for } I < I_k/20$$

$$P^B = a*I'(1-a*I'/(4*P^B m) \qquad \text{for } I_k/20 \leq I < 2*I_k$$

$$P^B = P^B m \qquad \text{for } 2*I_k \leq I$$

where a=alpha

P^B=production per unit of chlorophyll

I=irradiance

$I_k = P^B m/\text{alpha}$

$I' = (I - I_k/20)$

These production profiles are then integrated by this model to yield daily production estimates (mg $C.m^{-2}$).

Model Components

Chlorophyll a

Chlorophyll data were linearly interpolated for the depths required for the production calculation. If the data did not extend to the euphotic depth, I linearly regressed each chlorophyll profile and used the extrapolated values down to the euphotic depth.

Water Transparency

Daily water transparency profiles were extrapolated by the program by linearly regressing the $\log_{10}$ of the normalized submarine light measurements from 3 m to the maximun depth sampled. Data were normalized to the daily surface (0 m) reading. Rather than using the measurement taken just below the surface of the water (which is subject to error due to scattering of light by waves), the 0 m value was calculated by dividing the corresponding air measurement by 1.34, the immersion correction factor for the quantum sensor. In general, light extinction in the top 3 m was not log linear, and light measurements shallower than 3 m were not included in the regression.

The slope of the regression line is called the extinction coefficient (k). The regression line was extended to define the depth of the euphotic zone (Z_{EUPI}), defined here as the depth to which 0.5% of the surface light penetrated, which was calculated by:

$$Z_{EUPI}=\log_{10}0.005\text{-intercept/slope}$$

using the slope and intercept from the linear regression.

Chlorophyll and water transparency profiles were linearly interpolated to estimate values between sampling days, and the first and last sampling values in all input datasets were used to calculate production outside the sampling period.

Solar Radiation

Incoming solar radiation (insolation) data was modelled because empirical data was unavailable due to a malfuctioning strip chart recorder during the sampling period. Three light regimes were modelled for the sampling period. These regimes were used to calculate three estimates of total production as a function of insolation; maximum (cloudless), cloud cover corrected (based on twice daily on-site meteorological observations), and minimum (assuming continuous 10/10 cloud cover). The model is described in detail in Appendix A.

Statistical Treatment of Data

To test for the homogeneity of the water mass, more than one location was sampled on days when weather conditions permitted. These data (chlorophyll a and nutrients) were tested in a two-way analysis of variance (depth, location) for each sampling date. The results of this test showed there were no significant trends with depth or location ($p > 0.05$) i.e. that the water column appeared to be well mixed. For each variable measured a coefficient of variation (the standard deviation divided by the mean) was calculated for each date and averaged for the 6 replicate sampling days to indicate variability associated with the measurements (Table 1). Because the water column was well mixed, mean water column concentrations of the measured variables were reported. These variables were expressed as the mean $\pm$ 2 standard deviations. Standard error was not reported, since sample sizes varied.

The variables measured during the sampling period were tested to determine if changes in concentration or value increased, decreased or

showed no change with time. This was done using the General Linear Models (GLM) procedure from the Statistical Analysis System's (SAS) library, which computes a linear regression (Freund and Littell 1981). The null hypothesis was that there was no change in the concentration of chlorophyll, etc. with time. A statistical significance was recorded when the probability of rejecting the null hypothesis when it was true was 5% (i.e. when alpha was <= 0.05). The actual probabiliy is reported for each test.

To test whether the concentrations of the nutrients measured were related to chlorophyll a concentrations, the same statistical procedure (GLM) was used as above. Chlorophyll was the dependant variable, and the null hypothesis was that changes in nutrient concentration had no relationship to changes in chlorophyll a concentration, or that the slope of the regression line was zero.

A stepwise regression was done using the STEPREG procedure from the SAS library to determine the measured variable which accounted for the most variability in chlorophyll concentration. This was done to indicate a possible limiting factor in the growth of phytoplankton.

Table 1. Descriptive statistics for chlorophyll a and nutrients for days when more than one location was sampled. This was done to indicate the variability of measurements made at different depths at two or more locations.

a) Chlorophyll a

date (1982)	locations sampled	mean ($mg.m^{-3}$)	std. dev.	C.V.(%) (sd/mean)	S.E.	n	depths sampled (m)
5 Jul	E,F	1.93	0.48	24.9	0.15	10	0,2,5,10,20
20 Jul	L,M	2.87	0.75	26.1	0.24	10	0,2,5,10,20
2 Aug	R,S	1.54	0.21	13.6	0.06	12	0,2,5,7.5,10,15
5 Aug	T,U	1.07	0.14	13.1	0.04	10	0,2,5,10,20
16 Aug	X,Y	3.12	0.22	7.05	0.07	10	0,2,5,10,15
17 Aug	Z,AA,BB	2.01	0.40	19.9	0.10	15	0,2,5,10,20
				$\bar{x}$ =17.4			

b) Silica

date (1982)	locations sampled	mean ($umol.L^{-1}$)	std. dev.	C.V.(%) (sd/mean)	S.E.	n	depths sampled (m)
5 Jul	E,F	19.5	0.95	4.87	0.30	10	0,2,5,10,20
20 Jul	L,M	22.8	1.15	5.04	0.36	10	0,2,5,10,20
2 Aug	R,S	17.7	1.88	10.6	0.54	12	0,2,5,7.5,10,15
5 Aug	T,U	19.7	0.58	2.94	0.18	10	0,2,5,10,20
16 Aug	X,Y	12.4	0.35	2.82	0.11	10	0,2,5,10,15
17 Aug	Z,AA,BB	16.3	1.39	8.53	0.36	15	0,2,5,10,20
				$\bar{x}$ = 5.80%			

c) Total dissolved nitrogen (TDN)

date (1982)		locations sampled	mean ($umol.L^{-1}$)	std. dev.	C.V.(%) (sd/mean)	S.E.	n	depths sampled (m)
5	Jul	E,F	35.5	2.16	6.08	0.68	10	0,2,5,10,20
20	Jul	L,M	34.2	4.44	13.0	1.40	10	0,2,5,10,20
2	Aug	R,S	34.4	5.34	15.5	1.54	12	0,2,5,7.5,10,15
5	Aug	T,U	32.5	3.96	12.2	1.25	10	0,2,5,10,20
16	Aug	X,Y	24.4	1.54	6.31	0.49	10	0,2,5,10,15
17	Aug	Z,AA,BB	29.8	2.19	7.35	0.56	15	0,2,5,10,20
					$\bar{x}$ = 10.1%			

d) Total dissolved phosphorus (TDP)

date (1982)		locations sampled	mean ($umol.L^{-1}$)	std. dev.	C.V.(%) (sd/mean)	S.E.	n	depths sampled (m)
5	Jul	E,F,	2.18	0.08	3.67	0.02	10	0,2,5,10,20
20	Jul	L,M	2.21	0.14	6.33	0.04	10	0,2,5,10,20
2	Aug	R,S	2.07	0.11	5.31	0.04	12	0,2,5,7.5,10,15
5	Aug	T,U	2.17	0.08	3.69	0.02	10	0,2,5,10,20
16	Aug	X,Y	1.70	0.05	2.94	0.02	10	0,2,5,10,15
17	Aug	Z,AA,BB	1.95	0.06	3.08	0.02	15	0,2,5,10,20
					$\bar{x}$ = 4.17%			

e) Particulate nitrogen (PN)

date (1982)	locations sampled	mean ($umol.L^{-1}$)	std. dev.	C.V.(%) (sd/mean)	S.E.	n	depths sampled (m)
5 Jul	E,F	1.65	0.46	27.9	0.15	10	0,2,5,10,20
20 Jul	L,M	1.41	0.58	41.1	0.19	10	0,2,5,10,20
2 Aug	R,S	1.33	0.38	28.6	0.11	12	0,2,5,7.5,10,15
5 Aug	T,U	0.94	0.20	21.3	0.06	10	0,2,5,10,20
16 Aug	X,Y	2.81	0.61	21.7	0.20	10	0,2,5,10,15
17 Aug	Z,AA,BB	1.49	0.74	49.7	0.19	15	0,2,5,10,20
				$\bar{x}$ = 31.7%			

f) particulate phosphorus (PP)

date (1982)	locations sampled	mean ($umol.L^{-1}$)	std. dev.	C.V.(%) (sd/mean)	S.E.	n	depths sampled (m)
5 Jul	E,F	0.12	0.03	25.0	0.08	10	0,2,5,10,20
20 Jul	L,M	0.13	0.04	30.1	0.01	10	0,2,5,10,20
2 Aug	R,S	0.10	0.03	30.0	0.01	12	0,2,5,7.5,10,15
5 Aug	T,U	0.07	0.03	42.9	0.01	10	0,2,5,10,20
16 Aug	X,Y	0.20	0.02	12.2	0.01	10	0,2,5,10,15
17 Aug	Z,AA,BB	0.12	0.04	30.0	0.01	15	0,2,5,10,20
				$\bar{x}$ = 28.4%			

RESULTS

Chlorophyll a

Chlorophyll a concentrations ranged from 0.09 to 3.70 $mg.m^{-3}$ and there was a statistically significant increase in chlorophyll concentration during the sampling period ($p<0.0001$, $r^2=0.31$). From 30 May to 22 June the mean water column chlorophyll concentration was very low, 0.1 ± 0.02 mg m^{-3} ($x\pm2sd$). The concentration increased to 1.39 ± 0.30 mg m^{-3} by July 5 and for the next four weeks fluctuated about a mean of 2.38 mg m^{-3}(Fig. 8). Chlorophyll concentrations dropped in early August but peaked again sharply on August 14, reaching the maximum seasonal mean concentration of 3.70 ± 0.50 mg m^{-3}.

Early and late season chlorophyll concentrations were relatively constant with depth; there was some stratification in mid-summer, with chlorophyll maxima at or near the surface (Fig. 9).

Diatoms dominated samples taken from the 25-35 % light levels, consistently accounting for more than 90 % of the number of cells present. Fragillaria oceanica was numerically the most abundant diatom, and members of the genera Thallosiosira, Nitzschia, Peridinium, and a group of phytoflagellates were also present.

Figure 8. Chlorophyll a concentrations ($mg.m^{-3}$) in the water column from June to August, 1982. The mean concentration was calculated for each sampling day and the mean $\pm$ 2 standard deviations graphed.

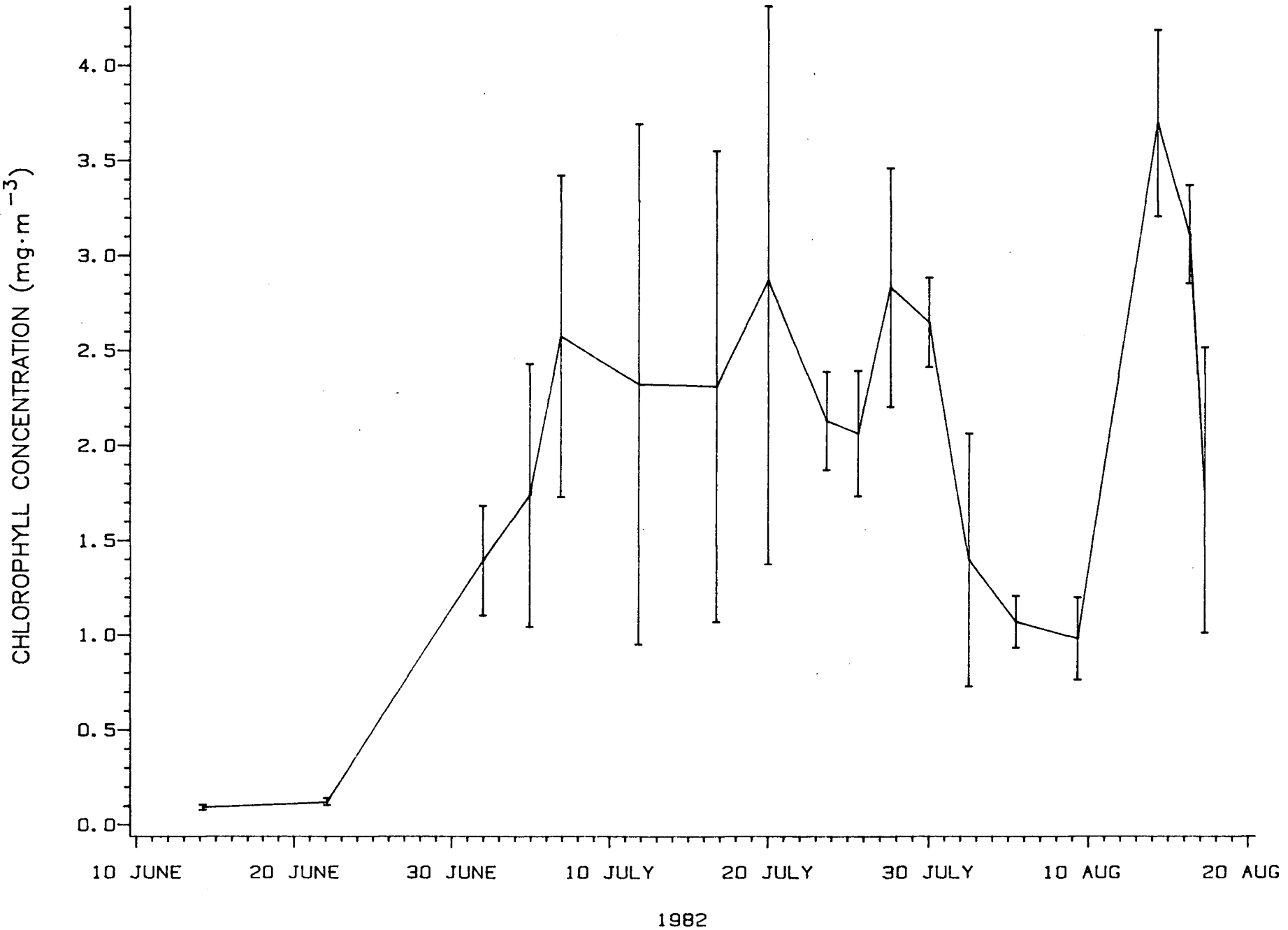
CHLOROPHYLL CONCENTRATION (mg·m⁻³)
4.0
3.5
3.0
2.5
2.0
1.5
1.0
0.5
0.0
10 JUNE
20 JUNE
30 JUNE
10 JULY
20 JULY
30 JULY
10 AUG
20 AUG
1982

Figure 9. Isopleth of chlorophyll a concentrations in the top 50 meters from June to August, 1982. There was a slight stratification of chlorophyll a in mid-summer, with higher concentrations near the surface.

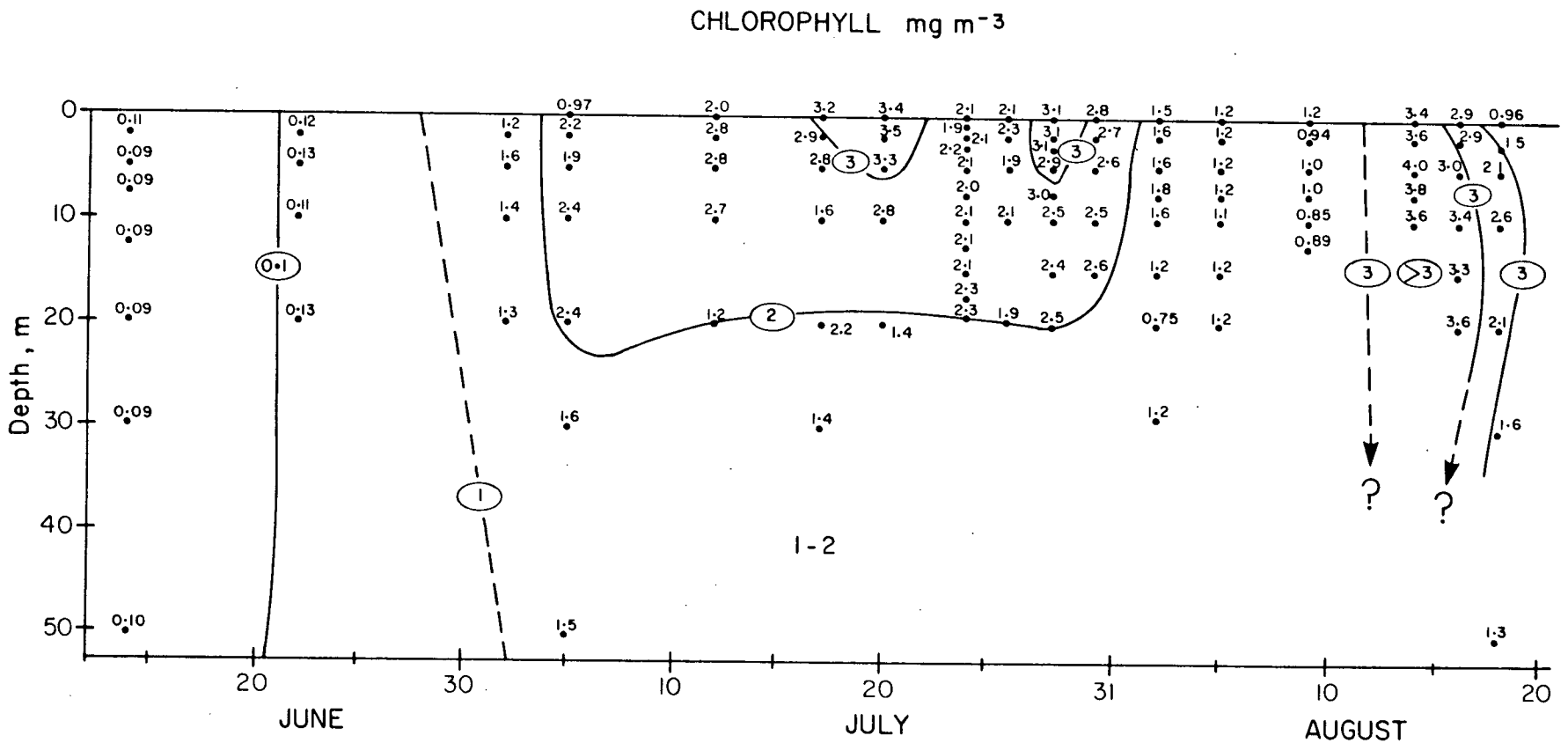
CHLOROPHYLL mg m⁻³
Depth, m
0
10
20
30
40
50
JUNE
JULY
AUGUST
20
30
10
20
31
10
20
0·1
1
2
3
1-2
?
?

Nutrient Chemistry

Silica

Soluble reactive silicon concentrations ranged from 11.6 to 24.8 umol.L^{-1}, with a mean concentration of 19.2±6.1 umol.L^{-1} (Fig. 10). From 30 May to 9 August, concentrations ranged from 17.7 to 22.8 umol.L^{-1} but marked changes occured from 9-17 August (Fig. 11). From 9 August to 14 August the mean silica concentration decreased from 21.9 to 11.7 umol.L^{-1}, then increased back to 18.4 umol.L^{-1} by 17 August. There was a statistically significant decrease in the concentration of silica with time ($p<0.0001$, $r^2=0.24$).

With the exception of 2 and 17 August, silica concentrations were relatively homogeneous with depth. There was little vertical stratification during the sampling period.

To compare relative concentrations over time, silica concentrations were normalized to the maximum concentration for each day (Si_{max}). With the exception of 17 July 2 August and 17 August, silica concentrations were generally 90-95% of Si_{max}, and the maximum concentration was usually at the maximum depth sampled (Fig. 12).

Nitrogen and Phosphorus

The first nitrogen and phosphorus samples were collected on 22 June. Low chlorophyll concentrations prior to and including 22 June suggest these macronutrients were also close to winter levels at this time.

The overall mean concentration of total nitrogen was 35 umol.L^{-1} (range 26-42 umol.L^{-1}). Total nitrogen (TN) was calculated by summing

Figure 10. Silica concentrations (umol.L^{-1}) in the water column from June to August, 1982. The mean concentration was calculated for each sampling day and graphed as the mean $\pm$ 2 standard deviations.

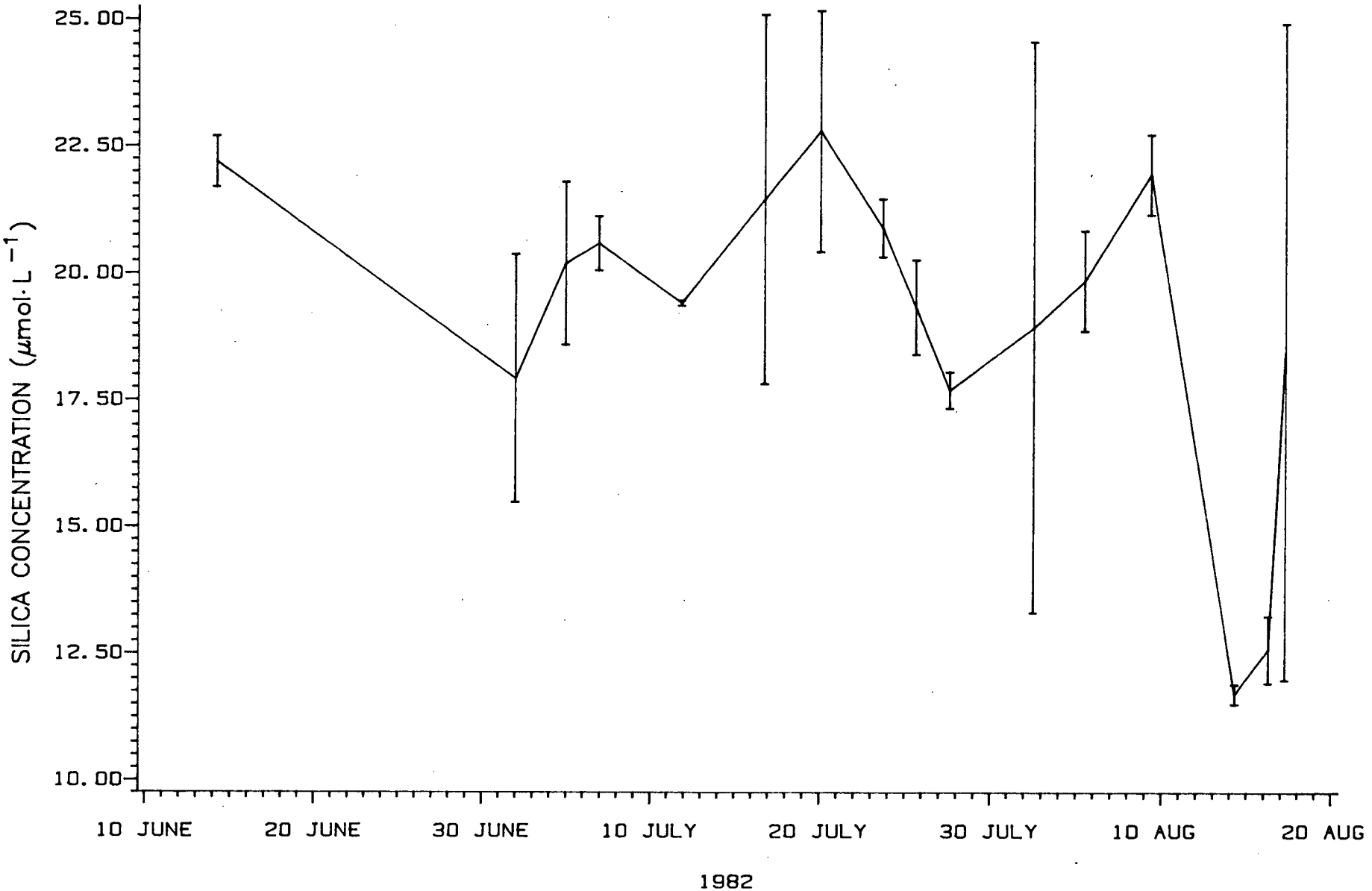
25.00
22.50
20.00
17.50
15.00
12.50
10.00
SILICA CONCENTRATION (μmol·L⁻¹)
10 JUNE
20 JUNE
30 JUNE
10 JULY
20 JULY
30 JULY
10 AUG
20 AUG
1982

Figure 11. Isopleth of silica concentrations (umol.L^{-1}) from June to August, 1982. Silica concentrations varied little with depth or during the sampling period.

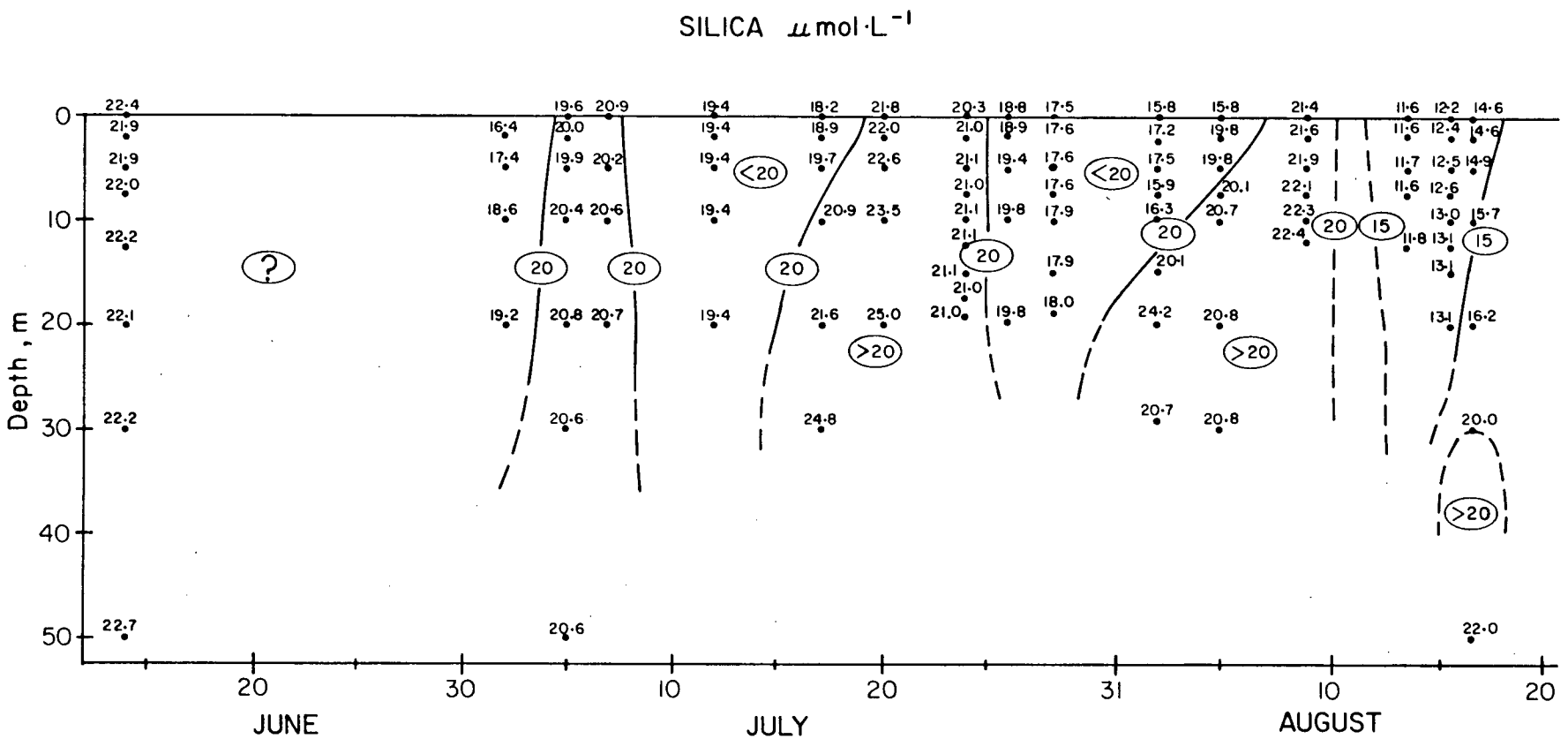
SILICA μmol·L⁻¹
Depth, m
0
10
20
30
40
50
JUNE
JULY
AUGUST
20
30
10
20
31
10
20
?
<20
20
>20
15

Figure 12. Isopleth of silica concentrations normalized to the maximum daily concentration. This isopleth shows that although silica concentrations did not generally change much in the top 50 meters, the maximum concentration was usually at the maximum depth sampled.

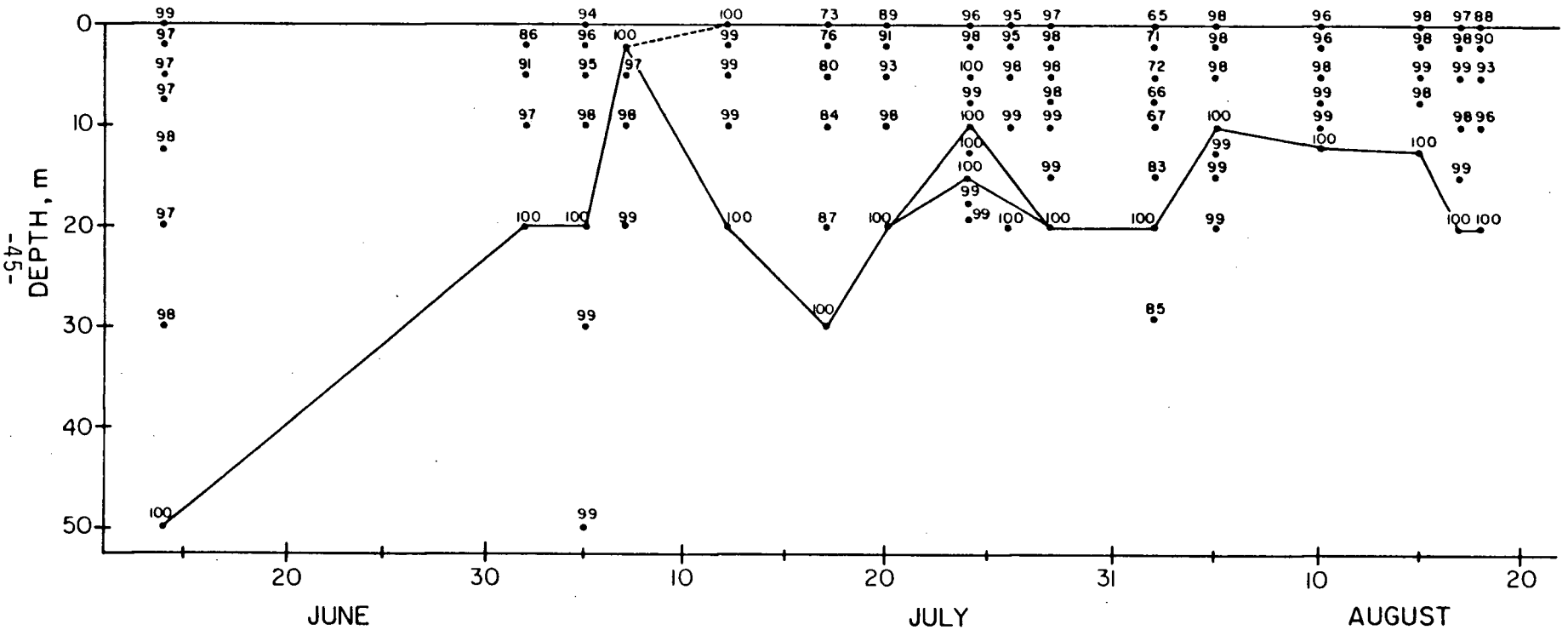
DEPTH, m
0
10
20
30
40
50
20
30
10
20
31
10
20
JUNE
JULY
AUGUST

total dissolved nitrogen, about 95% of TN, and particulate nitrogen (Fig. 13), about 5% of TN (Fig. 14). There was a statistically significant decrease in the total nitrogen concentration with time ($p<0.001$, $r^2=0.37$). A linear regression of chlorophyll with particulate nitrogen showed there was a statistically significant increase in chlorophyll concentration with increasing particulate nitrogen concentration, and this model accounted for 74% of the variance in particulate nitrogen ($p<0.0001$, $r^2=0.74$).

The seasonal pattern of phosphorus concentrations was similar to that of nitrogen. The mean concentration of total phosphorus was 2.13 ± 0.27 umol.L^{-1} (range 1.71 to 3.26 umol.L^{-1})(Fig. 15). Total dissolved phosphorus averaged approximately 95% of total phosphorus, and ranged from 1.68 to 3.04 umol.L^{-1}. There was a statistically significant decrease in total phosphorus with time ($p<0.0001$, $r^2=0.39$). A linear regression of chlorophyll with particulate phosphorus showed there was a statistically significant increase in chlorophyll concentration with increasing particulate phosphorus concentrations ($p<0.0001$, $r^2=0.73$). The mean concentration of particulate phosphorus was 0.12 umol.L^{-1} (Fig. 16).

To test for the dependency of chlorophyll a on nutrients, a stepwise multiple regression analysis of chlorophyll a with dissolved nutrients and date was computed (Table 2). This regression showed that 39% of the variation in chlorophyll a concentration was attributable to variations in silica concentration and that date and total dissolved nitrogen (TDN) and total dissolved phosphorus (TDP) concentrations were not important to the regression. Particulate nitrogen and phosphorus

Figure 13. Particulate nitrogen concentrations in the water column from June to August, 1982. The mean concentration was calculated for each sampling day, and the mean $\pm$ 2 standard deviations were graphed.

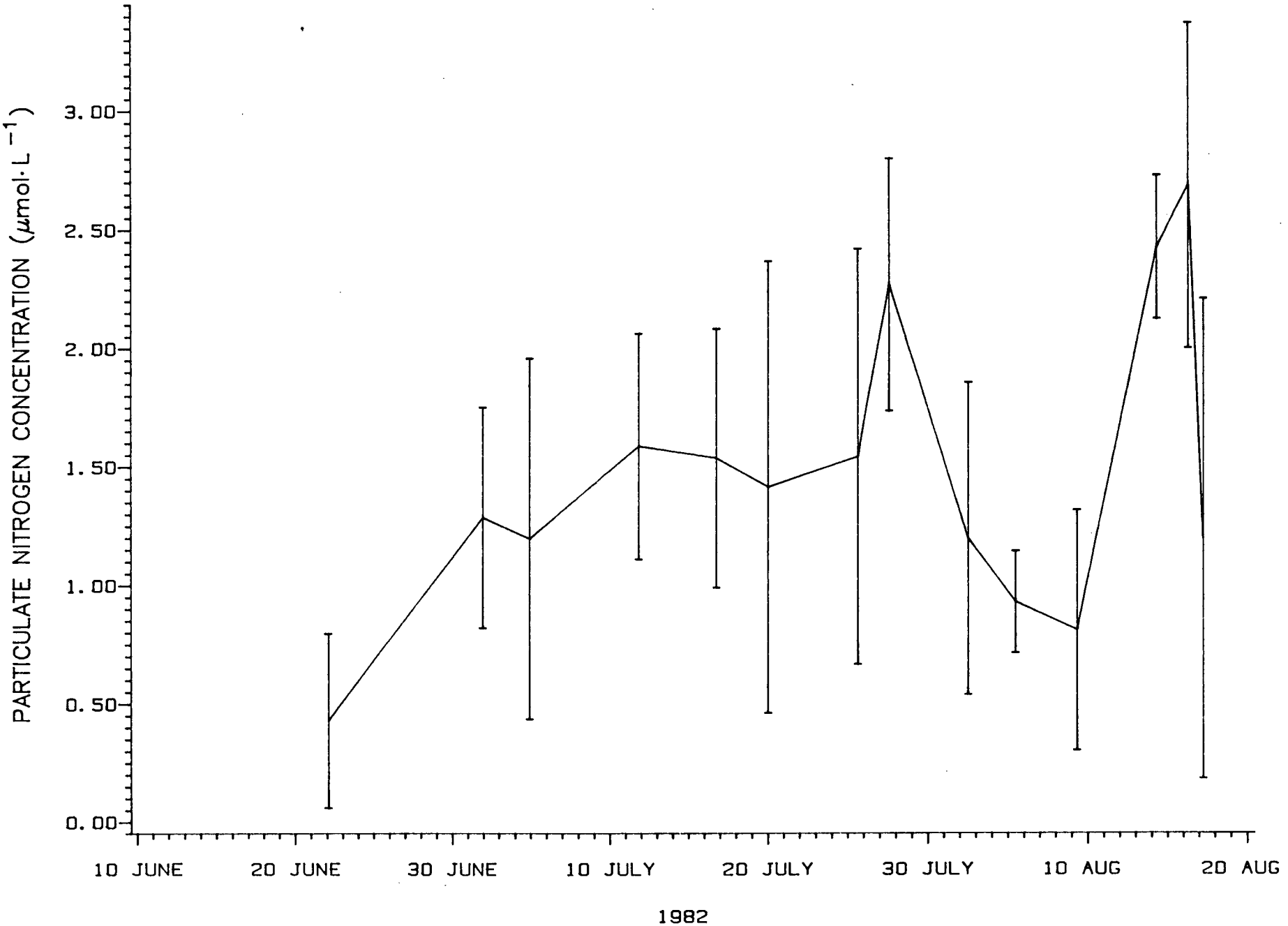
PARTICULATE NITROGEN CONCENTRATION (μmol·L⁻¹)
3.00
2.50
2.00
1.50
1.00
0.50
0.00
10 JUNE
20 JUNE
30 JUNE
10 JULY
20 JULY
30 JULY
10 AUG
20 AUG
1982

Figure 14. Total nitrogen concentrations in the water column from June to August, 1982. The mean concentration was calculated for each sampling day, and the mean $\pm$ 2 standard deviations were graphed.

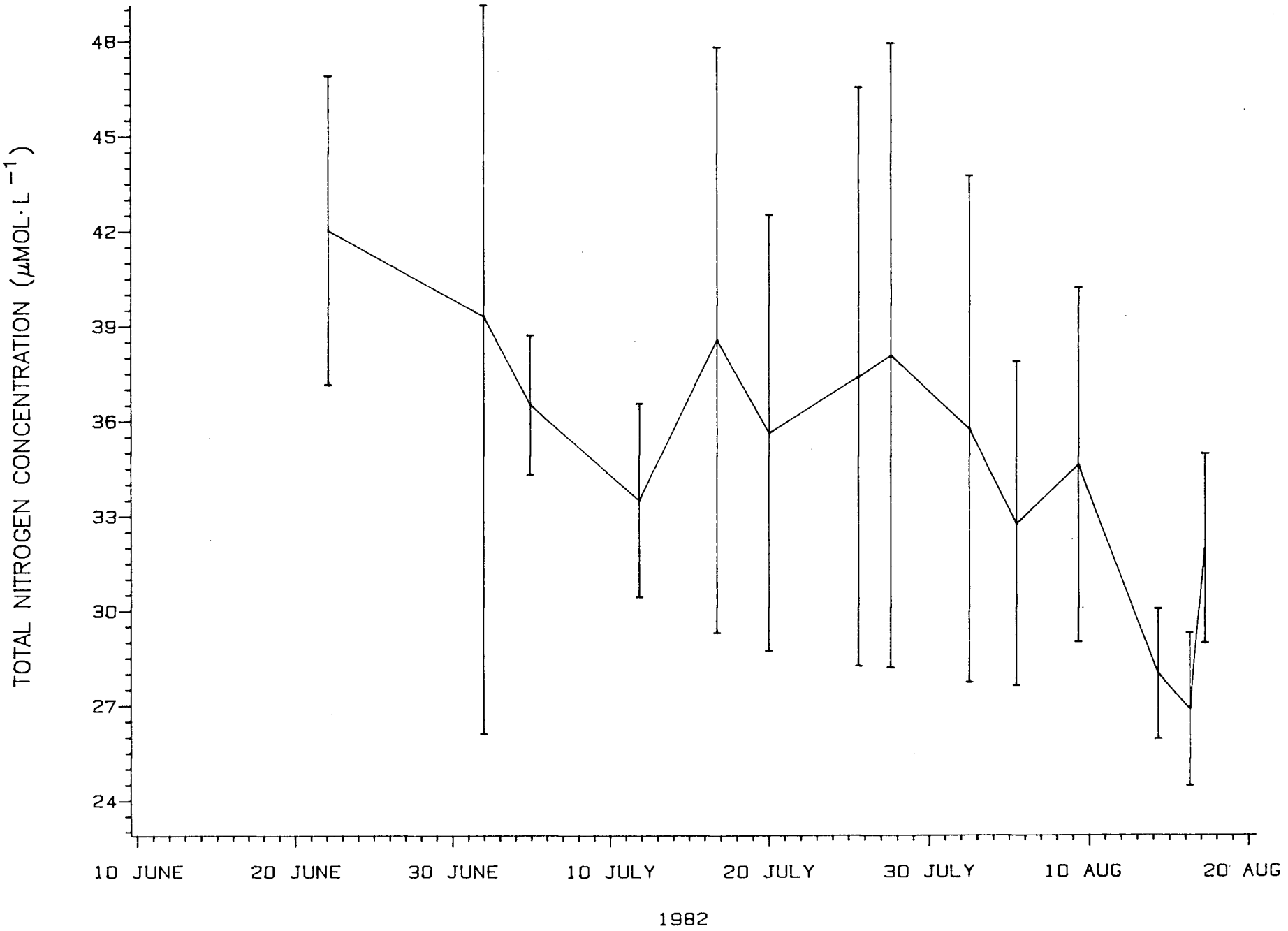
TOTAL NITROGEN CONCENTRATION (μMOL·L⁻¹)
48
45
42
39
36
33
30
27
24
10 JUNE
20 JUNE
30 JUNE
10 JULY
20 JULY
30 JULY
10 AUG
20 AUG
1982

Figure 15. Total phosphorus concentrations in the water column from June to August, 1982 (mean $\pm$ 2 standard deviations).

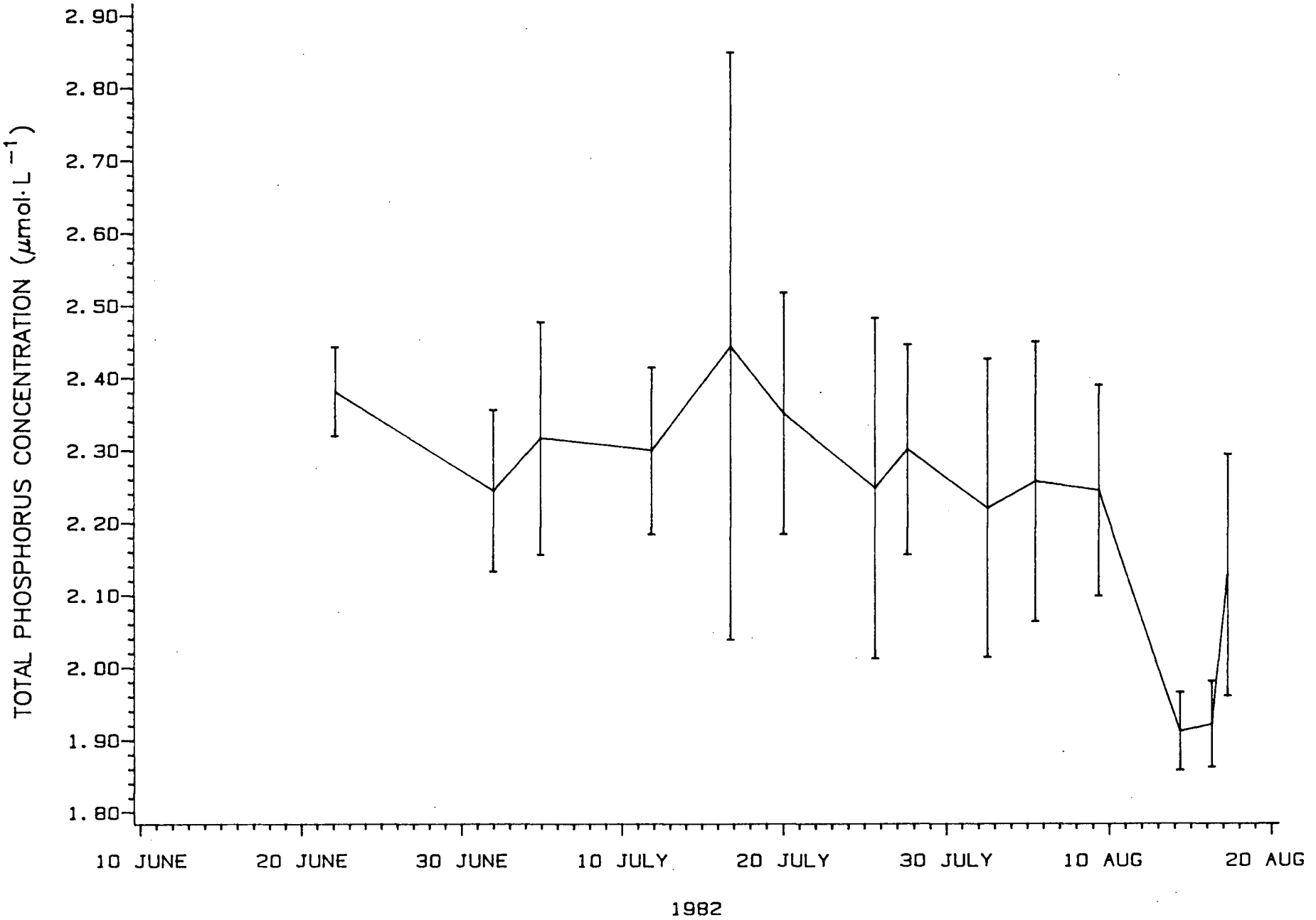
TOTAL PHOSPHORUS CONCENTRATION (μmol·L⁻¹)
2.90
2.80
2.70
2.60
2.50
2.40
2.30
2.20
2.10
2.00
1.90
1.80
10 JUNE
20 JUNE
30 JUNE
10 JULY
20 JULY
30 JULY
10 AUG
20 AUG
1982

Figure 16. Particulate phosphorus concentrations in the water column from June to August, 1982 (mean $\pm$ 2 standard deviations).

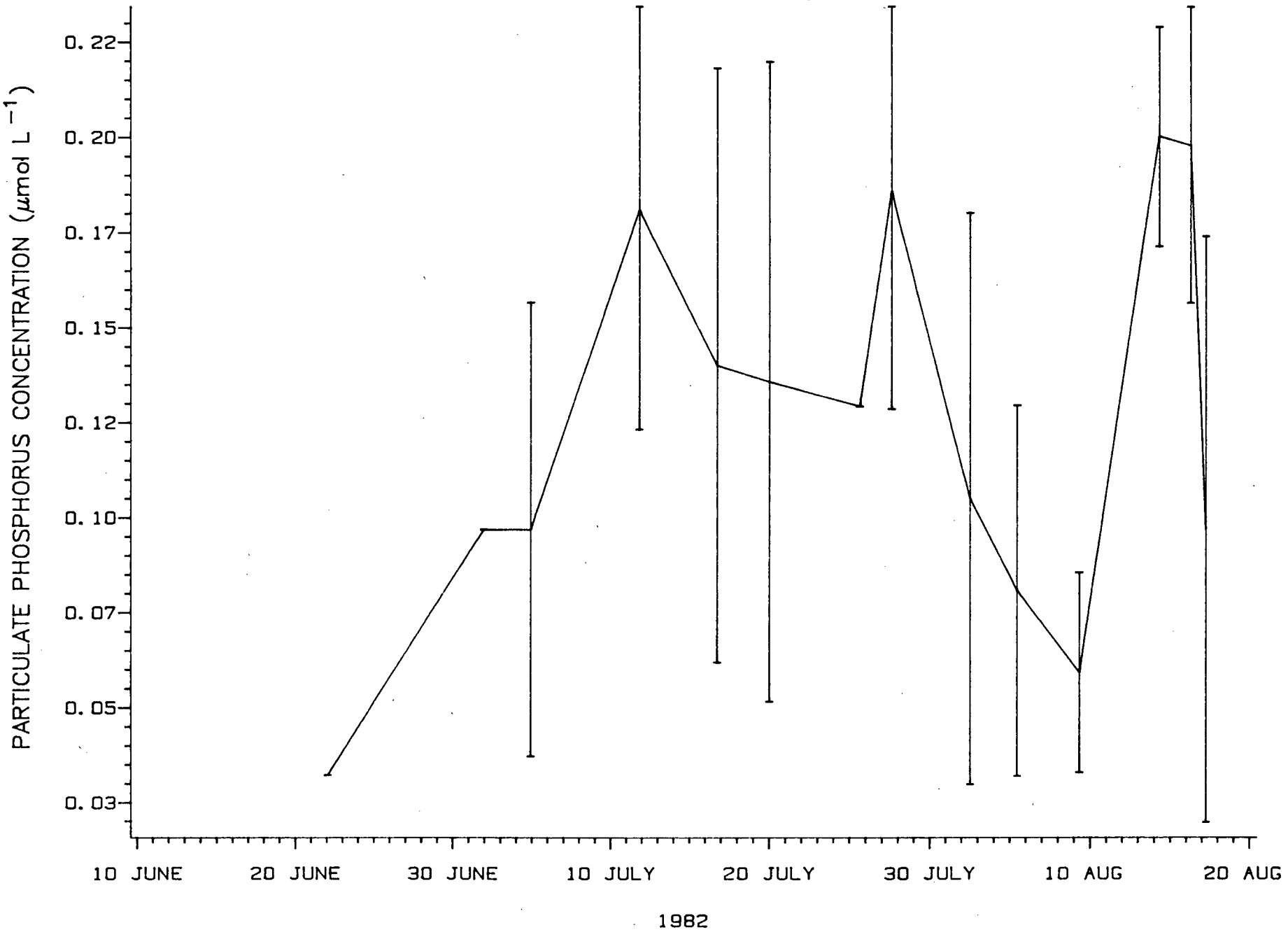
PARTICULATE PHOSPHORUS CONCENTRATION (μmol L⁻¹)
0.22
0.20
0.17
0.15
0.12
0.10
0.07
0.05
0.03
10 JUNE
20 JUNE
30 JUNE
10 JULY
20 JULY
30 JULY
10 AUG
20 AUG
1982

Table 2. Results of stepwise regression of chlorophyll a with dissolved nutrients and date. Changes in silica concentration accounted for 39% of the variability in chlorophyll a concentrations, and changes in time, TDN and TDP had little effect on changes in chlorophyll a concentration.

Step	Variable	R^2	Overall F
1	Silica	0.387	51.09
2	date	0.408	27.58
3	TDP	0.418	18.88
4	TDN	0.418	14.04

were not included in the regression because of the likely autocorrelation between these variables and chlorophyll a.

PHYSICAL OCEANOGRAPHY

Water transparency

Extinction coefficients ranged from -0.0377 m^{-1} on June 14 to -0.0908 m^{-1} on August 14, with a mean of -0.0566 m^{-1} (Fig. 17). There was a slight but statistically significant decrease ($p<0.0187$) in extinction coefficients (k) (increase in turbidity) with increasing chlorophyll concentration, although this model accounted for only 30% of the variation in k.

Euphotic zone

The mean depth of the euphotic zone was 39 m (range 22 to 53 m) (Fig. 18), and there was a statistically significant decrease in the depth of 0.5% surface light penetration with time ($p<0.0349$, $r^2=0.25$). A linear regression of euphotic depths with chlorophyll concentration showed a statistically significant decrease in the depth of the euphotic zone with increasing chlorophyll concentrations ($p<0.0144$, $r^2=0.32$). Chlorophyll concentrations accounted for only 32 % of the variation in euphotic depths; linear regressions of particulate nitrogen and phosphorus with euphotic depth showed that while particulate nitrogen concentrations were significantly related to euphotic depth ($p<0.0414$, $r^2=0.30$), chlorophyll concentrations accounted for slightly more variation. Particulate phosphorus concentrations were not significantly ($p<0.05$) related to euphotic depth.

Figure 17. The change in extinction coefficients from June to August, 1982.

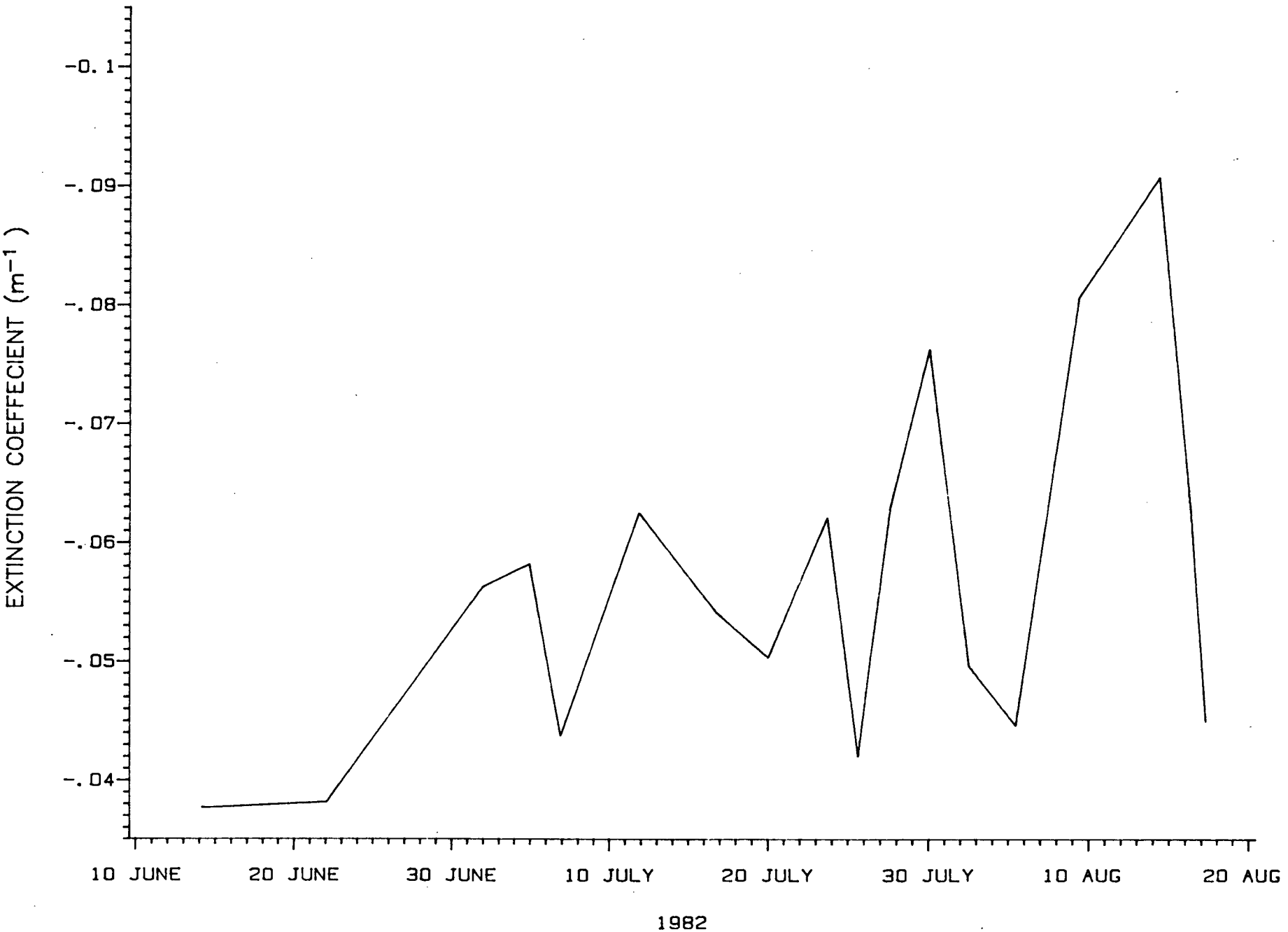
EXTINCTION COEFFECIENT (m^{-1})
-0.1
-.09
-.08
-.07
-.06
-.05
-.04
10 JUNE
20 JUNE
30 JUNE
10 JULY
20 JULY
30 JULY
10 AUG
20 AUG
1982

Figure 18. The euphotic depth, defined as the depth to which 0.5% of the surface light penetrates, from June to August, 1982. This depth was greatest (54 m) early in the season when the chlorophyll a concentrations were low, and was 22 m on 14 August during the second, and largest, phytoplankton bloom.

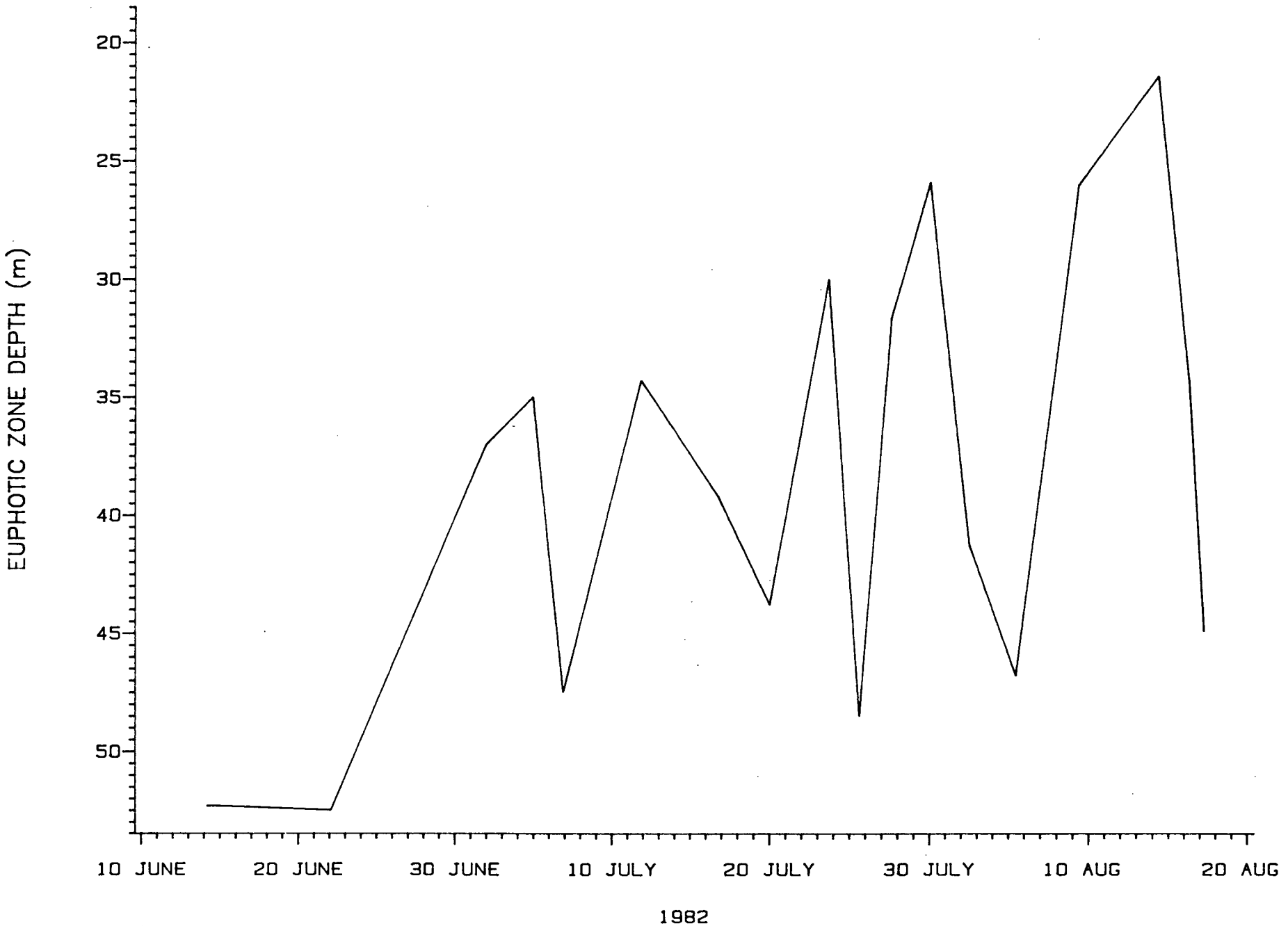
EUPHOTIC ZONE DEPTH (m)
20
25
30
35
40
45
50
10 JUNE
20 JUNE
30 JUNE
10 JULY
20 JULY
30 JULY
10 AUG
20 AUG
1982

Temperature, Salinity and Density

Water temperature and salinity showed no trends; they varied little with depth or time. The mean water column temperature was $-1.0\pm0.6^{o}C$, and ranged from -1.9 to $0.1^{o}C$. The mean salinity and density of the water column from 0 to 20 meters was 32.05 ± 1.39 ppt and 25.76 ± 1.11 $kg.m^{-3}$ respectively.

PRIMARY PRODUCTION

Alpha and $P^{B}m$

All the incubator data from the light saturation experiments were used to calculate alpha and $P^{B}m$ (Table 3).

Alpha, the slope of light-limited photosynthesis, ranged from 3.04 to 25.94 mg C/(mg chl.Einstein.m^{-2}) during the sampling period, and the overall mean was 8.54 mg C/(mg chl.E.m^{-2})(Fig. 19). A frequency diagram of these values showed that 90% were between 3 and 14 mgC/(mg chl.Einstein.m^{-2}) (Fig. 20). $P^{B}m$, the maximum rate of photosynthesis per unit of chlorophyll, ranged from 1.44 to 4.01 mg C/(mg chl.h^{-1}); the mean $P^{B}m$ was 2.73 mg C/(mg chl.h^{-1}) (Figs. 21,22).

The mean values of alpha and $P^{B}m$ were used in primary production calculations because linear regressions of these parameters with depth and time showed no statistically significant depth or seasonal trends ($p<0.05$).

Primary Productivity

Primary productivity was calculated for the three light regimes modelled (Appendix A) from 1 June to 17 August, 1982 (Table 4).

Table 3. Descriptive statistics for alpha and $P^{B}m$.

Parameter	Mean	Std dev	S.E.	Median	n
alpha	8.54	5.56	0.98	6.70	32
$P^{B}m$	2.73	0.71	0.13	2.56	32

Figure 19. Alpha values (mg C/(mg Chl.E^{-1}.m^{-2})) obtained from photosynthesis-light experiments.

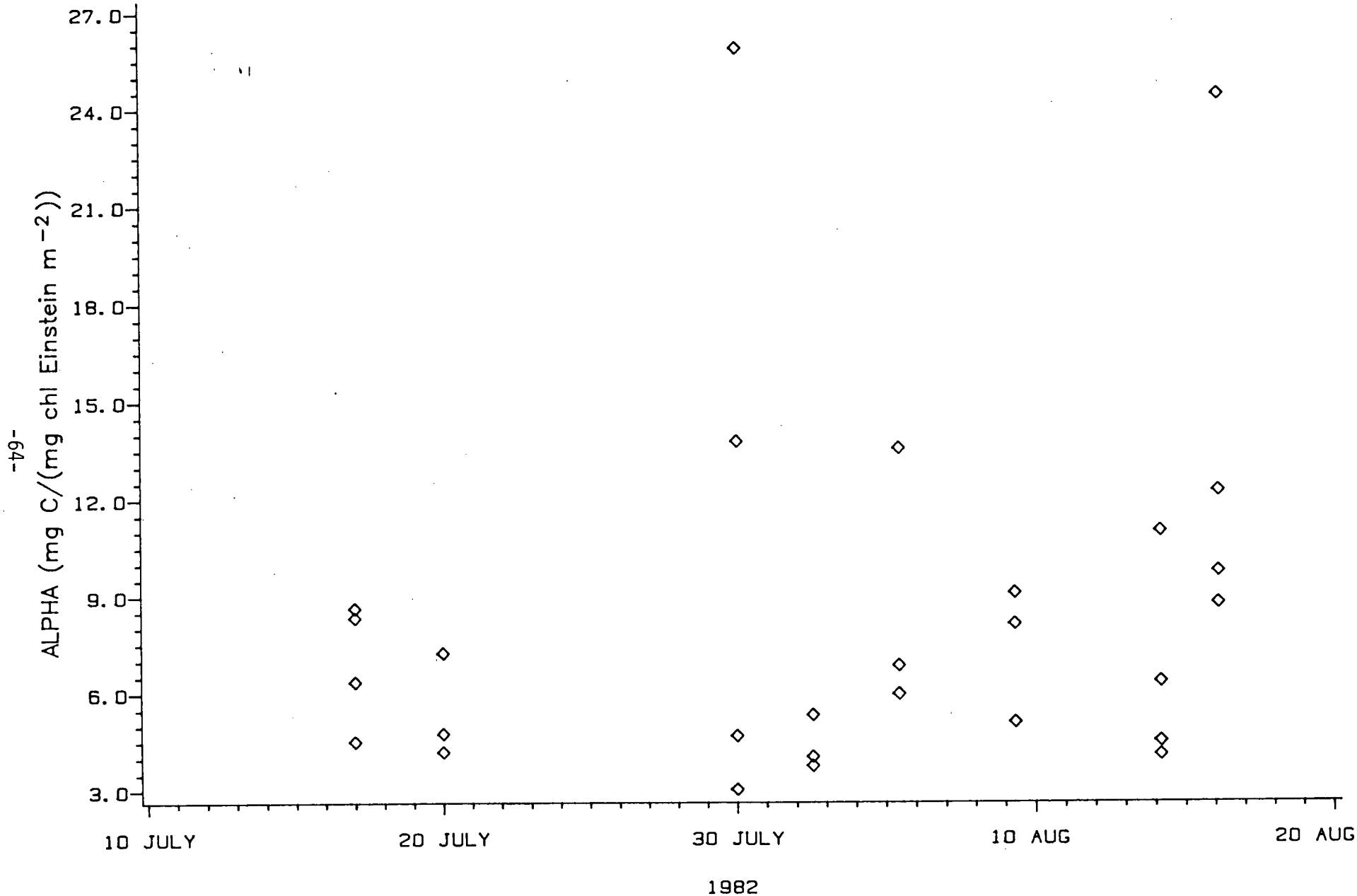
27.0
24.0
21.0
18.0
15.0
12.0
9.0
6.0
3.0
ALPHA (mg C/(mg chl Einstein m^{-2}))
10 JULY
20 JULY
30 JULY
10 AUG
20 AUG
1982

Figure 20. A frequency diagram of alpha values.

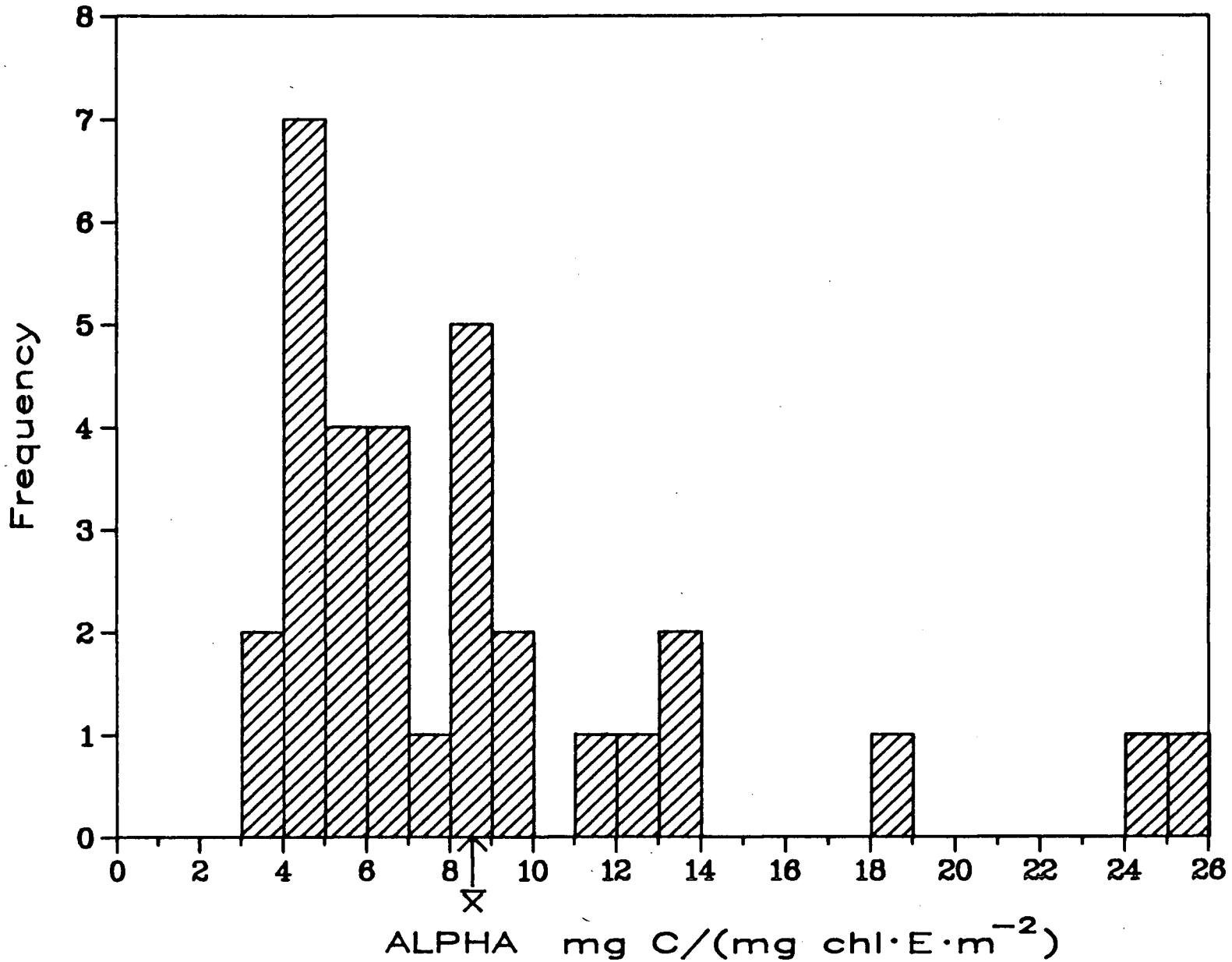
Frequency
0
1
2
3
4
5
6
7
8
0
2
4
6
8
10
12
14
16
18
20
22
24
26
X̄
ALPHA mg C/(mg chl·E·m⁻²)

Figure 21. $P^{B}m$ values (mg C/(mg chl.h^{-1})) obtained from photosynthesis-light experiments.

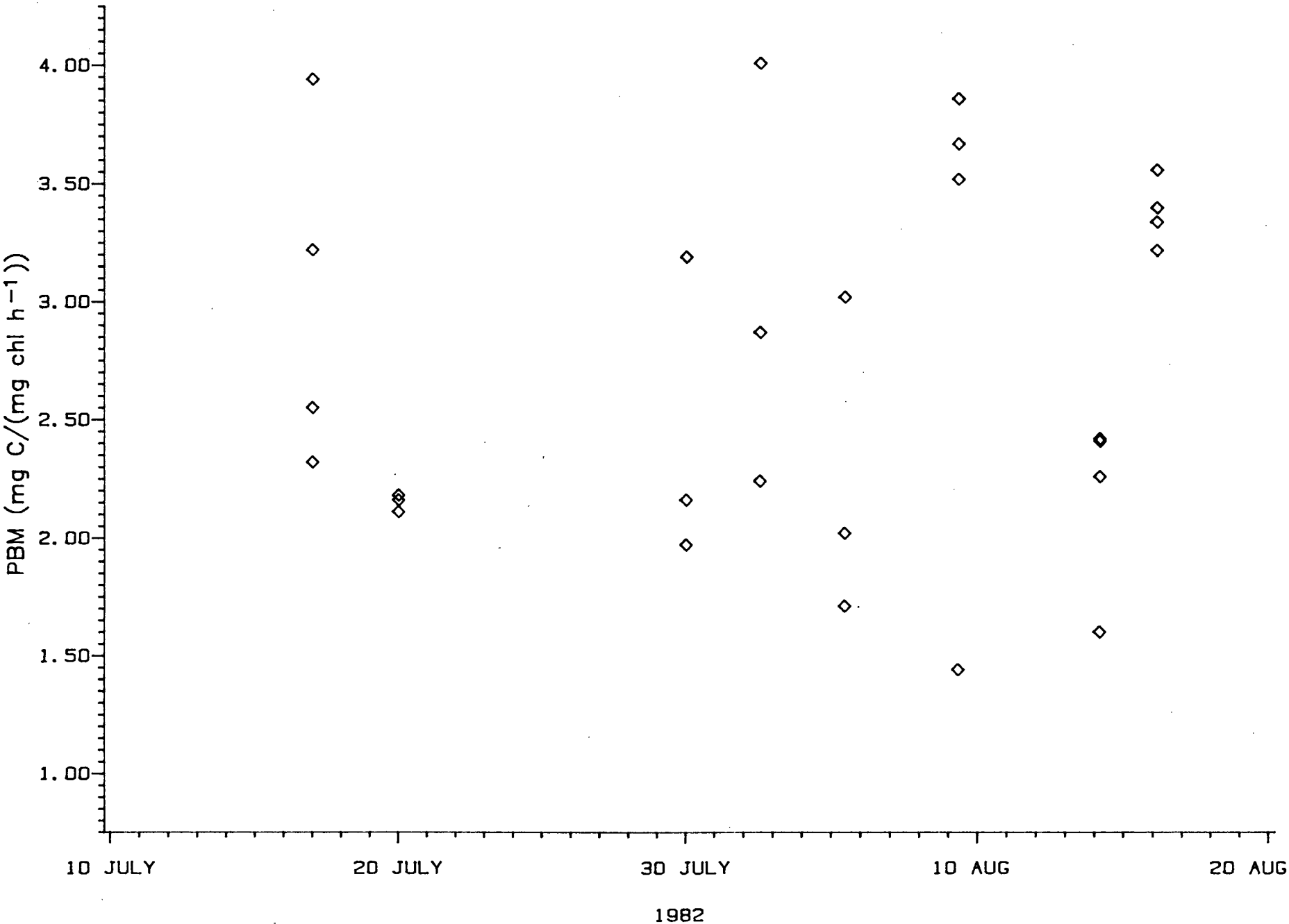
PBM (mg C/(mg chl h^{-1}))
4.00
3.50
3.00
2.50
2.00
1.50
1.00
10 JULY
20 JULY
30 JULY
10 AUG
20 AUG
1982

Figure 22. Frequency diagram of $P^{B}m$ values.

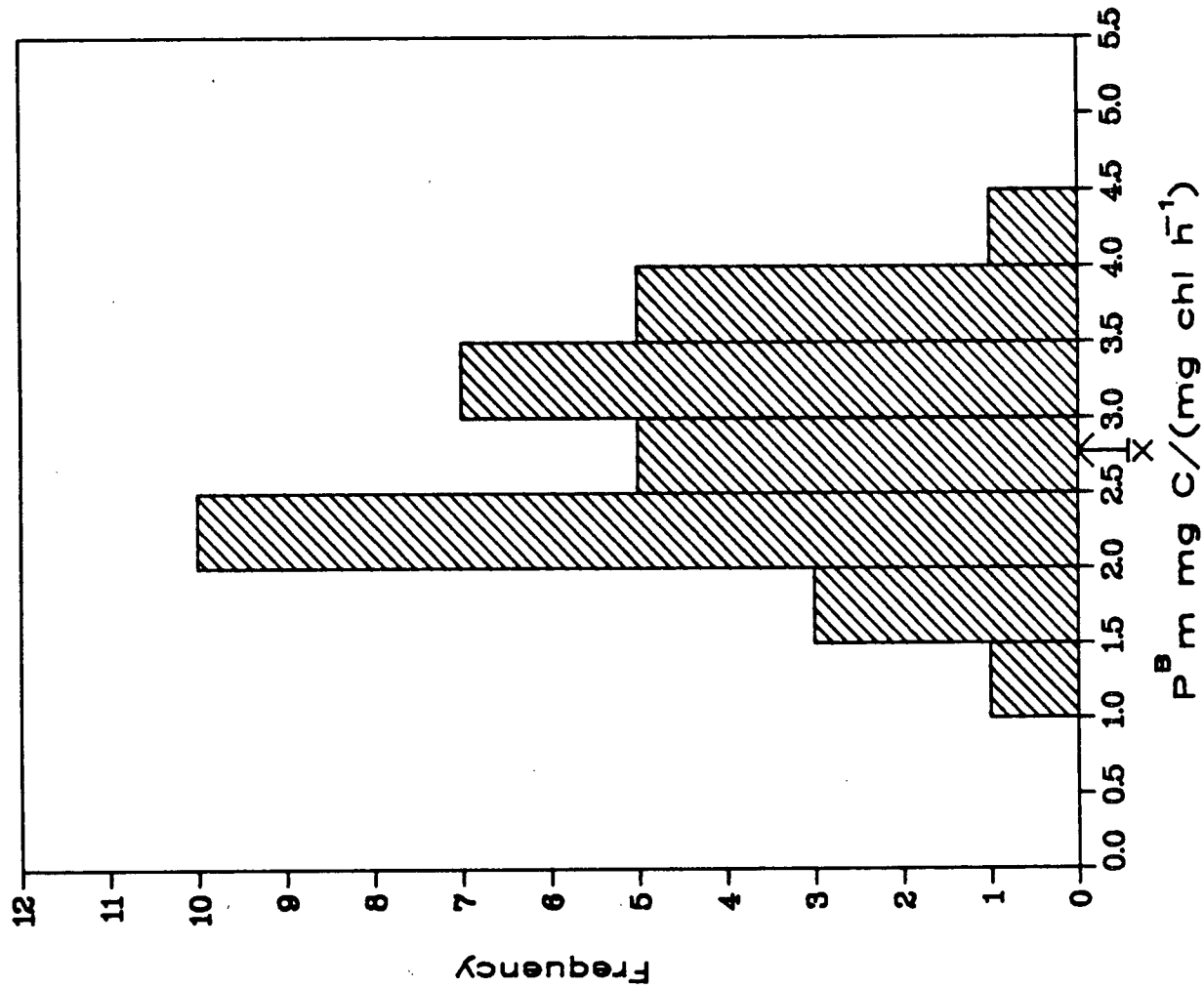
Frequency
0
1
2
3
4
5
6
7
8
9
10
11
12
0.0
0.5
1.0
1.5
2.0
2.5
3.0
3.5
4.0
4.5
5.0
5.5
$\bar{X}$
P^B_m mg C/(mg chl h^{-1})

Early season productivity averaged approximately 0.09 g $C.m^{-2}.day^{-1}$. With cloud-corrected solar radiation, the two peaks of productivity during the sampling period were 2.5 g $C.m^{-2}.day^{-1}$ on 20 July and 2.3 g $C.m^{-2}.day^{-1}$ on 13 August. The plots of production vs time using the three light regimes (Fig. 23) show the highest peak of productivity occured on 20 July .

Figure 23. Integrated primary production (mg $C.m^{-2}$) calculated with maximum, cloud-cover corrected, and minimum solar radiation values from June to August, 1982.

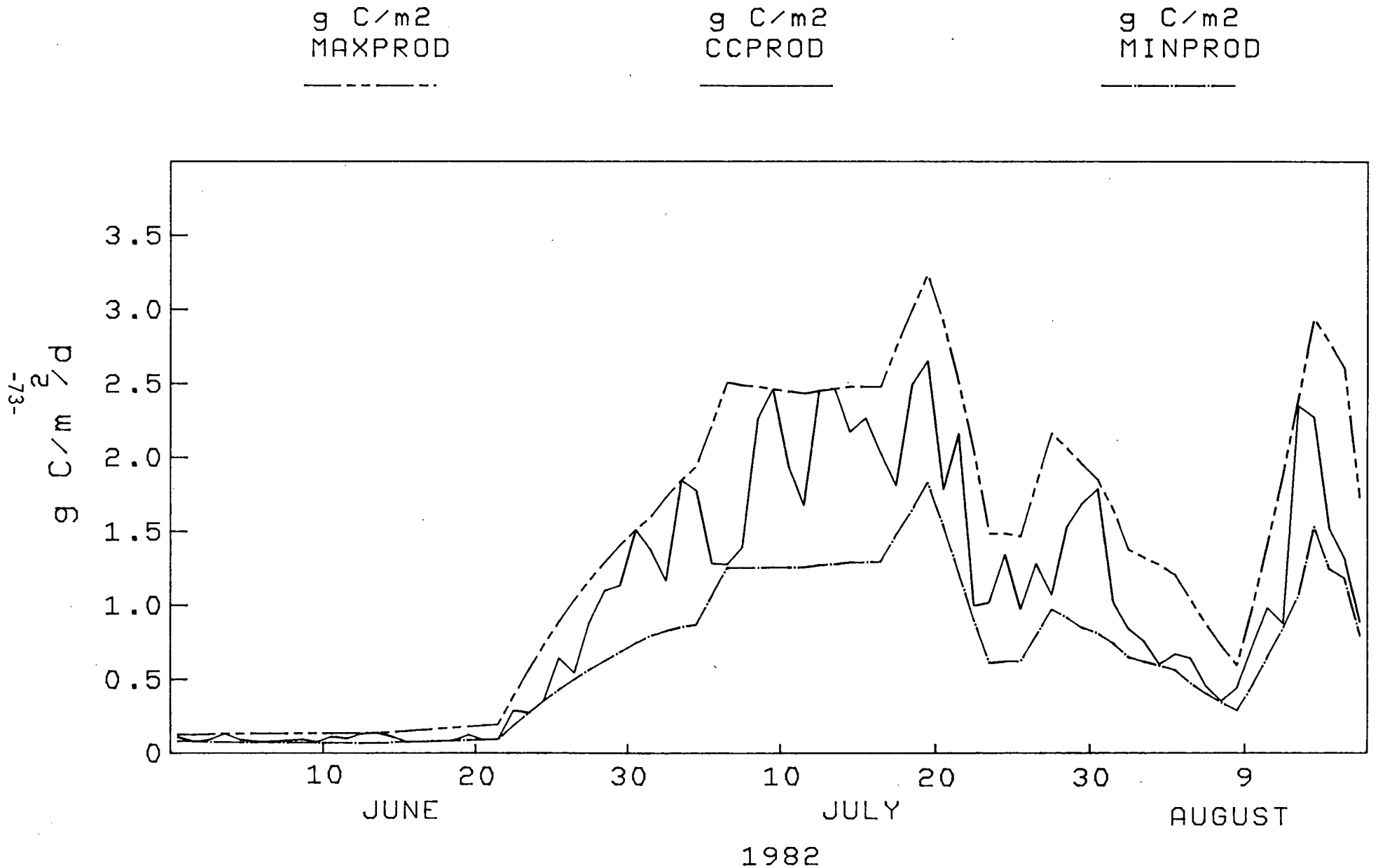
g C/m2
MAXPROD
g C/m2
CCPROD
g C/m2
MINPROD
g C/m2/d
3.5
3.0
2.5
2.0
1.5
1.0
0.5
0
10
20
30
10
20
30
9
JUNE
JULY
AUGUST
1982

Table 4: Primary productivity calculated from 1 June to 17 August, 1982, using maximum, cloud-corrected, and minimum solar radiation values. (alpha=8.54 mg C/(mg chl.Einstein.m^{-2}, $P^{B}m$=2.73 mg C /(mg chl.h^{-1}).

g C.m^{-2}		
Maximum(cloudless)	Solar Radiation Cloud-corrected	Minimum(10/10 overcast)
106	77.9	51.5

DISCUSSION

Chlorophyll a

From the end of May until late June, the concentration of chlorophyll was low (0.09 mg chl m^{-3}) and distributed evenly in the top 50 m. Early season concentrations were within the range of winter values at Resolute Bay, 0.001 to 0.1 mg chl.m^{-3} (Welch and Kalff 1975) and somewhat lower than those at Frobisher Bay in mid-June 1963, 0.3 mg chl. m^{-3}(Grainger 1979).

Chlorophyll concentrations peaked twice, with the first peak occuring from 20-30 July and the second peak, larger than the first and of much shorter duration, occuring between 9-15 August. The overall mean of 72 mg chl m^{-2} (1.85 mg chl.m^{-3}) is comparable to values reported for northern regions such as Lancaster Sound (Borstad and Gower 1985) Baffin Bay (Harrison et al. 1982) and Resolute Bay (Welch and Kalff 1975).

Nutrients

The concentrations of soluble reactive silica, total dissolved nitrogen (TDN) and total dissolved phosphorus (TDP) were highest early in the season (late June) when chlorophyll concentrations were low (0.09 mg chl.m^{-3}). There were statistically significant decreases in the

concentrations of these three nutrients during the summer and a statistically significant increase in chlorophyll concentration. This suggests that nutrients were being consumed by phytoplankton and were appearing as particulate nitrogen and phosphorus, which were positively correlated with chlorophyll concentration. The stepwise regression showed that the depletion of silica was greater than the depletion of TDN and TDP, but it is unlikely that silica concentrations were ever limiting, since the largest change in the concentration of silica was during the second phytoplankton bloom, and it only decreased by half during that time. The low nutrient concentrations which develop in surface waters during or after bloom conditions in such areas as Frobisher Bay (Grainger 1975) and Baffin Bay (Harrison et al. 1982) did not occur in Fram Sound. This suggests that nutrients were being injected into the system, probably by the upwelling of deeper water. Vertical profiles of temperature, salinity and nitrogen, phosphorus and silica concentrations indicate that the water column was well-mixed for the entire sampling period.

Silica

Early season silica concentrations were about 20 umol.L^{-1}, slightly lower than the spring values of 25 to 30 umol.L^{-1} recorded in Jones Sound from 1961-1963 (Apollonio 1976b). The most geographically comparable silica data are from an Arctic cruise in August and September, 1977; a mean silica concentration in Fram Sound of 22 umol.L^{-1} from 50 to 200 m with vertical stratification in the top 50 m ranging from 10.8 umol.L^{-1} near the surface to 20 umol.L^{-1} at 50 m was

reported (Jones and Coote 1980). The lowest silica concentrations I measured, 11.7 and 12.6 umol.L^{-1}, occured on 14 August and 16 August respectively during the second phytoplankton bloom. These concentrations are still considerably higher than other workers have measured in late summer, for example 2-5.2 umol.L^{-1} in the top 10 m in late July in Jones Sound (Apollonio 1976b), and 2.87 umol.L^{-1} in the Baffin Bay mixed-layer in late August to mid-September (Harrison et al. 1982). These data indicate that silica is probably re-supplied by local upwelling conditions in Fram Sound. Slight vertical stratifictaion was evident on the last sampling day (17 August 1982). The data of Jones and Coote (1980) suggests that stratification may occur, although silica depletion probably does not proceed in Fram Sound to the low concentrations of other Arctic areas sampled to date.

Nitrogen and Phosphorus

Total nitrogen concentrations ranged from 26 to 42 umol.L^{-1}. Because most nitrogen measurements in Arctic waters are of nitrate (NO_3^-) and ammonia (NH_4^+), comparisons with geographically similar nitrogen data are not possible. The only available nitrate data for Fram Sound was measured in August and September 1977, and two locations were sampled. Nitrate concentrations were somewhat stratified, with surface concentrations of 10 and 14 umol.L^{-1} respectively (Jones and Coote 1980). These concentrations were comparable to those reported for Lancaster Sound (12 umol.L^{-1}, Jones and Coote 1980) and considerably higher than those found in the Baffin Bay mixed layer (0.15 umol.L^{-1}, Harrison et al. 1982).

Particulate nitrogen and chlorophyll concentrations showed similar trends during the season. A linear regression of these two variables showed chlorophyll accounted for 74% of the variance in particulate nitrogen concentrations suggesting that particulate nitrogen can serve as an index of phytoplankton biomass in the absence of chlorophyll data.

If the same water mass was sampled for the entire sampling period the total nitrogen concentrations should remain essentially constant, but the concentration of total nitrogen decreased during this time. This is likely due to either depletion of particulate nitrogen by sinking or zooplankton grazing, or to water masses passing the sampling area with different concentrations of total nitrogen.

Phosphorus, like nitrogen, was measured as total dissolved phosphorus (TDP) and particulate phosphorus (PP); measurements of phosphate (PO_4^{3-}) cannot be extracted from TDP and PP values without additional data. Late summer phosphate data from Fram Sound showed that phosphate was relatively homogeneous to 150 m with a mean concentration of 1.6 $umol.L^{-1}$ (Jones and Coote 1980). This concentration is comparable to late summer Baffin Bay mixed layers (1.2 $umol.L^{-1}$, Harrison et al. 1982) and Lancaster Sound (1.7 $umol.L^{-1}$, Jones and Coote 1980).

PHYSICAL OCEANOGRAPHY

The euphotic zone is defined as the depth to which 1.0% or 0.5% of the surface light penetrates. The mean depth of the euphotic zone during the sampling period was 39 m (defined using 0.5%), which is comparable to the depth of 34 m for Baffin Bay in late summer (Harrison

et al. 1982). The linear regression of euphotic depth with chlorophyll a showed a statistically significant inverse relationship, although chlorophyll accounted for only 32% of the variance. This suggests that other factors are affecting water transparency, such as the seasonal bloom of zooplankton associated with changes in chlorophyll concentration, or that the 'noise' associated with low chlorophyll measurements obscured the relationship.

The temperature and salinity data indicated that the water column was well mixed to the maximum depth sampled throughout the sampling period. This is consistent with the vertical profiles of nutrient and chlorophyll data, which were also homogeneously distributed. The low salinity surface layer reported to develop in other Arctic areas was not observed in Fram Sound. The water from Norwegian Bay was well mixed by the action of the set and tidal currents in Hell Gate, Cardigan Strait and Fram Sound, and this vertical instability due to mechanical forces prevented the formation of a low salinity surface of melt-water.

PRIMARY PRODUCTION

Primary production and phytoplankton biomass data are sparse for the eastern Canadian Arctic (Harrison et al. 1982, Borstad and Gower 1985, Welch and Kalff 1975, Apollonio 1976b). In Baffin Bay, phytoplankton biomass (chlorophyll a) and primary production rates averaged 57 mg chl.m^{-2} (1.26 mg.m^{-3}) and 227 mg C.m^{-2}.d^{-1} during the summer of 1978; large chlorophyll maxima (about 6 times greater than surface concentrations) were consistantly measured at or near the bottom of the euphotic zone (Harrison et al. 1982). Although nitrate

concentrations were low in the euphotic zone, Harrison et al. (1982) detected no apparent signs that nutrients limited production and concluded that nutrient concentrations may not be as important as previously believed in controlling Arctic primary production (Dunbar 1968). Strong subsurface chlorophyll maxima were also present in Jones Sound just below the pycnocline in August, 1979, where chlorophyll was up to 18 $mg.m^{-3}$ and the average concentration was 1.97 mg $chl.m^{-3}$ (69 mg $chl.m^{-2}$) (Borstad and Gower 1985). Phytoplankton biomass reached a maximum concentration of 100 mg $chl.m^{-2}$ (15 $mg.m^{-3}$) in Resolute Bay during August 1972, and the total annual production was estimated at 45 g $C.m^{-2}.yr^{-1}$ (Welch and Kalff 1975). The only winter chlorophyll measurements to date in the Lancaster Sound area were also taken at Resolute Bay and were below 0.1 mg $chl.m^{-2}$ (Welch and Kalff 1975). In Frobisher Bay, about 1500 km southeast of Resolute Bay, total annual production was approximately 40 and 70 g $C.m^{-2}.yr^{-1}$ in 1968 and 1969; the difference in production between these two years was associated with seasonal differences in sea ice cover and hence light availability (Grainger 1975). Chlorophyll concentrations were somewhat higher in Frobisher Bay than Resolute Bay in August, ranging from 10-200 mg $chl.m^{-2}$ in 1969, and nitrate, which became depleted in August, was thought to limit primary production at that time (Grainger 1975).

The average production rate during the sampling period of the present study, calculated with cloud-cover corrected insolation, was 998 mg $C.m^{-2}.d^{-1}$ (26 mg $C.m^{-3}.d^{-1}$). This is a considerably higher rate of production than reported by other workers for Arctic waters, although there are no comparable primary production rates available for Arctic

polynyas (Dunbar 1981).

I calculated primary production rates for maximum and minimum solar radiation to provide a range of rates relating to insolation. These rates were 1.5 g $C.m^{-2}.d^{-1}$(maximum) and 0.76 g $C.m^{-2}.d^{-1}$ (minimum), and the cloud-cover corrected and minimum solar radiation production rates were 72 % and 45% of the maximum insolation respectively. These calculations assume that the slope of light-limited photosynthesis (alpha) on a P-I curve does not change with changes in ambient light and that nutrients are not limiting, i.e. that light is the only limiting factor.

The production rates reported by other workers for Arctic waters were determined by a variety of techniques; comparisons between photosynthetic rates measured by in-situ incubations or shore-based incubations with different incubator designs, using ^{14}C-uptake or oxygen evolution methods, are probably not entirely valid. Recent preliminary work comparing two incubator designs yielded somewhat different photosynthetic rates (Welch et al. unpub. data).

The high rate of production I calculated for Fram Sound was largely due to the magnitude of alpha and $P^B m$, which were 8.54 mg C/(mg chl.E.m^{-2}) and 2.73 mg C/(mg chl.h^{-1}) respectively. The only available comparative alpha and $P^B m$ data for Arctic waters, 2.97 mg C/(mg chl.E.m^{-2}) and 1.22 mg C/(mg chl.h^{-1}), are considerably lower than these values (Platt et al. 1982). These measurements were made in Baffin Bay and the water samples were taken from the 50% light level. These data are not strictly comparable with those of the present study, since different incubator designs and incubation techniques were used. I

incubated 60 ml samples on rotating clear acrylic disks at 5 light levels, whereas Platt et al. (1982) statically incubated 1 ml samples at 50 light levels. The effect of different incubation techniques on the outcome of alpha and $P^B m$ is currently being investigated (Brian Irwin, pers comm).

The lowest values of alpha and $P^B m$ measured in Fram Sound, 3.04 mg C/ (mg chl.E.m^{-2}) and 1.44 mg C/(mg chl h^{-1}), were higher than the mean values from the 50 % light level in Baffin Bay, which were 2.97 mg C/(mg chl.E.m^{-2}) and 1.22 mg C/(mg chl.h^{-1})(Platt et al. 1982). The difference between the alpha values in the two locations could be due to physiological differences between the two algal populations, differences in experimental design and techique, or a combination of both.

A high alpha value indicates the phytoplankton have a high 'photosynthetic effeciency'. Further work must be done to determine if phytoplankton in such a turbulant system as Hell Gate-Cardigan Strait Polynya and Fram Sound are more photosynthetically efficient than those from more vertically stable locations.

Conclusion

Fram Sound is part of the Hell Gate-Cardigan Strait polynya, an area kept relatively ice-free year round by the combined effects of strong set and tidal currents and high winds. The results of the present study show the water column was well-mixed in this area; nutrients were continuously supplied and alpha and $P^B m$ values were higher than in less turbulant areas, where nutrients become depleted in the stable surface layer after a phytoplankton bloom. Chlorophyll a

concentrations were generally homogeneously distributed in Fram Sound, whereas in other Arctic areas subsurface chlorophyll maxima usually develop. The high primary productivity measured in the study area suggests that secondary productivity may also be higher here and/or downstream of this and other polynyas in summer.

LITERATURE CITED

Apollonio, S. 1976b. Primary production in the Canadian Arctic Archipelago, 1961-1963. Unpublished manuscript. Bigelow Laboratory for Ocean Sciences. Contribution No. 76016. 46 p.

Beaufort Sea Hydrocarbon Production and Transportation Proposal. 1984. Report to the Environmental Assessment Panel. Minister of Supply and Services Canada.

Borstad, G.A. and J.F.R. Gower. 1985. Phytoplankton chlorophyll distribution in the eastern Canadian Arctic. Arctic 37(3):224-233.

Dahlgren, L. 1974. Solar radiation climate near sea level in the Canadian Arctic Archipelago (Arctic Institute of North America, Devon Island Expedition 1961-1962). Ph.D. thesis, Uppsala University, Sweden.

Dunbar, M. J. 1968. Ecological developements in polar regions; a study in evolution. Prentice-Hall,Inc.,Englewood Cliffs,N.J. 119 p.

Dunbar, M. J. 1981. Physical causes and biological significance of polynyas and other open water in sea ice. In: I. Stirling and H. Cleator (ed.) Polynyas in the Canadian Arctic, Occasional paper 45, Canadian Wildlife Service.

Fee, E.J. 1984. Freshwater Institute Primary Peoduction Model User's Guide. Can. Tech. Rep. Fish. Aquat. Sci. 1328. 36 p.

Freund, R.J. and R.C. Littell. 1981. SAS for linear models: a guide to the ANOVA and GLM procedures. SAS Institute Inc.

Grainger, E.H. 1975. A marine ecology study in Frobisher Bay, Arctic Canada. In: Cameron, T.W.M. and L.W. Billingsley (ed.) Energy Flow-Its Biological Dimensions, A Summary of the IBP in Canada 1964-1974. 338 p.

Grainger, E.H. 1979. Primary production in Frobisher Bay, Arctic Canada. In: M.J. Dunbar (ed.) Marine Production Mechanisms International Biological Programme 20.

Harrison, W.G., T. Platt, and B. Irwin. 1982. Primary production and nutrient assimilation by natural phytoplankton populations of the eastern Canadian Arctic. Can. Journ. Fish. Aquat. Sci. 39:335-345.

International Oceanographic Tables Volume 1. 1972. Published jointly by the National Institute of Oceanography of Graeat Britian and the United Nations Educational, Scientific and Cultural Organization (UNESCO).

Jassby, A.D., and T. Platt. 1976. Mathematical Formulation of the relationship between photosynthesis and light for phytoplankton.

Limnology and Oceanography 24(4):540-547.

Jerlov, N.G. and E. Steemann Nielsen (ed). 1974. Optical Aspects of Oceanography. Academic Press, London and New York.

Jones, E.P., and A.R. Coote. 1980. Nutrient distributions in the Canadian Archipelago: indicators of summer water mass and flow characterictics. Can. Journ. Fish. Aquat. Sci. 37:589-599.

Le Grand, Y. 1968. Light, Colour and Vision. Chapman and Hall Ltd. London. Second Edition. 564 p.

Luning, K. 1981. Light. p 326-355. In: The Biology of Seaweeds. C.S. Lobban and and M.J. Wynne (ed). The University of California Press, Berkeley. (Botanical Monographs-Vol 17.)

McCree, K.J. 1972. Test of current definitions of photosynthetically active radiation against leaf photosynthesis data. Agric. Meteor. 10:443-453.

Milne, A.R. and B.D. Smiley. 1978. Offshore Drilling in Lancaster Sound: Possible Environmental Hazards. Dept. of Supply and Services Canada.

Parsons, T.R., M. Takahashi, and B. Hargrave. 1977. Biological Oceanographic Processes. Pergammon Press, 332 p.

Platt, T., W.G. Harrison, B. Irwin, E.P. Horne, and C.L. Gallegos. 1982. Photosynthesis and photoadaptation of marine phytoplankton in the Arctic. Deep Sea Research 29:1159-1170.

Raymont, J.E.G. 1980. Plankton and productivity in the oceans. Volume 1- Phytoplankton. Second edition. Pergammon Press. 489 p.

Sailing Directions, Arctic Canada. 1982. Vol. 1, Third edition. Dept. Fisheries and Oceans. Supply and Services Canada.

Schindler, D.W., R.V. Schmidt, and R.A. Reid. 1972. Acidification and bubbling as an alternative to filtration in determining phytoplankton production by the ^{14}C method. J. Fish. Res. Board Can. 29:1627-1631.

Shearer, J.A., E.R. DeBruyn, D.R. DeClerq, D.W. Schindler, and E.J. Fee. 1985. Manual of Phytoplankton Primary Production Methodology. Can Tech. Rep. Fish. Aquat. Sci.1341.

Smith, M., and B. Rigby. 1981. Distribution of polynyas in the Canadian Arctic.In I. Stirling and H. Cleator (ed.) Polynyas in the Canadian Arctic, Occas pap. 45, Canadian Wildlife Service.

Stainton, M.P., M.J. Capel, and F.A.J. Armstrong. 1977. The Chemical Analysis of Fresh Water, Second Edition. Can. Fish. Mar. Serv. Misc.

Spec. Publ. 25, 180 p.

Steeman Nielsen, E. 1952. The use of radiocactive carbon (C-14) for measuring organic production in the sea. J. Cons. Explor. Mer 18:117-140.

Stirling, I. 1981. The biological importance of polynyas in the Canadian Arctic. Arctic 33:303-315.

Szeicz, G. 1974. Solar radiation for plant growth. J. Applied Ecol. 11:617-636.

Taylor, A. 1964. Geographical Discovery and Exploration in the Queen Elizabeth Islands. Memoir 3, Geographical Branch, Mines and Technical Survey, Ottawa. 172 p.

Topham, D. R.,R.G. Perkin, S.D. Smith, R.J. Anderson, and G. Den Hartog. 1983. An investigation of a polynya in the Canadian Archipelago,I, Introduction and Oceanography. Journal of Geophysical Research. Vol.88, No. C5, pp 2888-2899.

Vollenweider, R.A. 1969. [Ed] A Manual on methods for measuring primary production in aquatic environments. IBP Handbook No.12, Blackwell Scientific Publications, Oxford and Edinburgh. 213 p.

Vowinckel, E. and S. Orvig. 1962. Relation between solar radiation income and cloud type in the Arctic. Jour. Appl. Meteor. 1:552-559.

Welch, H.E., and J. Kalff. 1975. Marine metabolism at Resolute Bay, N.W.T.. p 69-75.In Proceedings of the Circumpolar conference on Northern Ecology. National Research Council, Ottawa.

APPENDIX A

SOLAR RADIATION MODELS

Dahlgren (1974) made numerous measurements and observations of the solar radiation climate at Truelove Lowland (Devon Base Camp), Devon Island, N.W.T. ($75^{o}40'$N lat. $84^{o}32'$W long.) in 1961 and 1962. From these measurements and observations he derived the atmospheric coefficients necessary to calculate normal values of global radiation with a clear sky. He used direct solar radiation measurements made under cloudless, cloudy (less than 10/10 cover), and dense overcast conditions to derive empirical cloud cover correction factors and to verifiy and supplement the insolation (incoming solar radiation) values computed for different sky conditions.

I used these data and meteorological (cloud cover) observations recorded from May to August, 1982 to calculate insolation at Cape Vera ($76^{o}14'$N lat.98^{o} 13'W long.) under cloudless, cloudy and dense overcast conditions. These three datasets were then used in the primary production model to calculate primary production.

Assumptions of the Model

Dahlgren's data were collected twenty years ago, but the proximity of Truelove Lowland to Cape Vera and the geographical similarities between these locations rendered these data most suitable for estimating

insolation at Cape Vera (Fig. A.1). To use his data, I made the following assumptions: 1) Dahlgren's data represent 'typical' meteorological conditions at Truelove Lowland in 1961 and 1962, 2) the atmospheric conditions have not changed significantly in the High Arctic since 1961/62, and 3) the summer of 1982 at Cape Vera was 'typical' meteorologically.

Cape Vera is approximately 5^{o} longitude west of Truelove Lowland, which means local noon (the time when the sun is highest in the sky) occurs about 20 minutes later at this location than at Truelove Lowland. This difference was considered negligible and was not corrected for in the model.

Dahlgren's data collection and treatment

I will briefly describe the aspects of Dahlgren's work pertinent to the solar radiation model, followed by how I used these data to estimate insolation at Cape Vera.

Dahlgren measured instantaneous clear sky radiation simultaneously with filter measurements made with an Angstrom pyrheliometer to determine the transmission properties of the air. He measured these properties, Angstrom's turbidity coefficient, Linke's turbidity factor and the amount of precipitable water in the atmosphere, at different times of the day from February to October to characterize the atmospheric conditions on a daily and seasonal basis. Knowing these values, and having data for the intensity of direct solar radiation in an ideal atmosphere (an atmosphere without water vapor and aerosol particles) from other workers, Dahlgren calculated direct, clear sky

Figure A.1. Map of Jones Sound, showing the proximity of Truelove Lowland, where Dahlgren (1974) measured solar radiation, with Cape Vera.

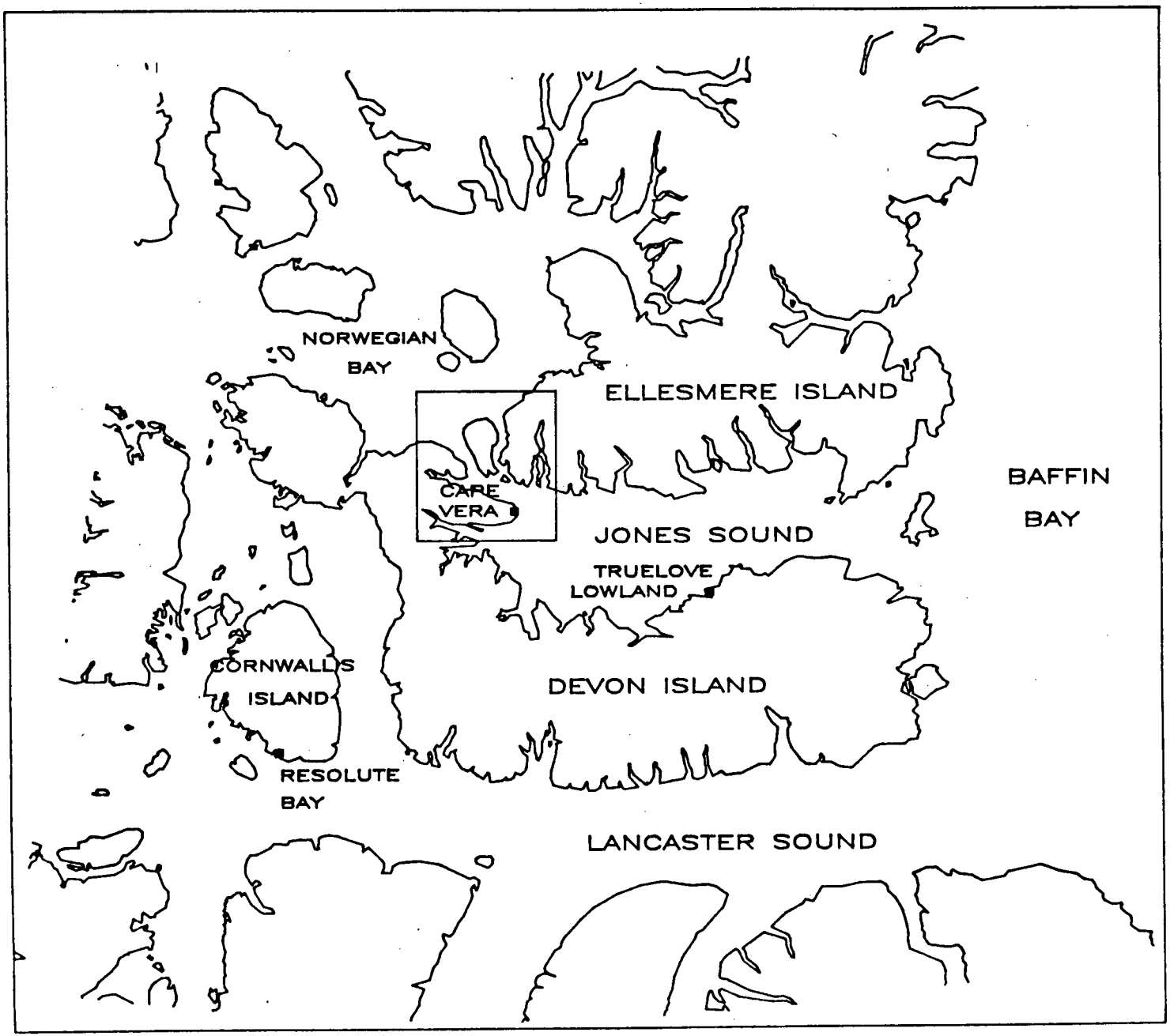
NORWEGIAN
BAY
ELLESMERE ISLAND
CAPE
VERA
BAFFIN
BAY
JONES SOUND
TRUELOVE
LOWLAND
CORNWALLIS
ISLAND
DEVON ISLAND
RESOLUTE
BAY
LANCASTER SOUND

insolation as a function of solar altitude. He also calculated diffuse radiation as a function of solar altitude and turbidity, both with high albedo (snow-covered ground) and with a lower albedo (ground bare of snow).

Global radiation (g_0), which consists of direct and diffuse radiation, was calculated from the following equation:

$$g_0 = I \sin h + d$$

where g_0=instantaneous global clear sky radiation (mcal $cm^{-2}min^{-1}$)

I =intensity of direct solar radiation

h =solar altitude

d =diffuse radiation

From these data, Dahlgren constructed monthly curves of global radiation as a function of solar altitude from February to October. He also made 470 measurements of the global clear sky radiation during these months, and they were usually in close agreement with his calculated values. These curves were necessary in order to calculate the total amount of global clear sky radiation received at this location each day.

Dahlgren computed daily totals of global clear sky insolation for every fifth day from 28 January to 14 November, during which period the sun was above the horizon for part or all of the day. This was done by calculating the solar altitude for even hours before and after local noon and, from the monthly curves of g_0 versus solar altitude,

determining the global clear sky insolation at that time. These values were graphed; they defined the shape of the diurnal curve. Daily insolation with a clear sky (G_0,cal.cm^{-2}. day^{-1}) was then calculated by graphic integration (Table A.1).

Cloud cover

Dahlgren also measured instantaneous solar radiation with a dense overcast (10/10 dense cloud cover), denoted g_{10}, in which case the global radiation consisted only of diffuse radiation. He made these measurements with different cloud types and calculated relative insolation,g_{10}/g_0, as a function of time and cloud type. From these values he developed curves relating the effect of cloud type and month on the amount of insolation recieved and also meaned all the cloud type values for each month to estimate a monthly mean value of relative insolation for all cloud types (Fig. A.2).

Estimation of insolation at Cape Vera

The purpose of estimating incoming solar radiation at Cape Vera was to provide mean half-hourly instantaneous insolation values from 1 June to 17 August. These data were then input to a primary production model (Fee, 1984) to calculate primary productivity at the south end of the Hell Gate-Cardigan Strait Polynya during this time.

Clear sky model

The following steps were taken to compute the clear sky insolation:

1) The data from Table 1 were linearly interpolated to provide insolation values from 00^{00} to 12^{00} h for the missing days.

Table A.1. Global radiation with a clear sky at actual solar distance.

g_0 = global radiation (mcal/cm^{2}min) with a clear sky

G_0 = daily insolation (ly/day) with a clear sky (daily total of global radiation)

D = daily insolation (ly/day) from a clear sky (daily total of diffuse radiation)

Hour angle = True solar time −12^h	g_0 mcal/cm^2 min													Sun on horizon	g_0 = 0	Daily insolation G_0	D	D/G_0
	00	01	02	03	04	05	06	07	08	09	10	11	12	h m	h m	ly/day	ly/day	%
Jan 28	0														0 00	0	0	-
Feb 8	14	8	2											0 00	2 46	2.0	2.0	100
10	25	17	5											1 12	2 59	4.1	4.0	98
15	49	43	20	4										2 16	3 36	10.7	7.7	72
20	86	77	49	14	1									3 01	4 10	22.0	12.8	58
25	137	122	86	43	7									3 40	4 40	38.9	19.2	49
Mar 1	166	152	115	64	18	1								4 08	5 06	51.9	25.2	49
5	203	188	146	88	31	5								4 35	5 31	66.9	31.2	47
10	261	246	203	137	64	16								5 07	6 01	95.9	39.5	41
15	316	301	258	192	111	36	7							5 38	6 32	127.5	49.0	38
20	373	358	314	251	163	73	18							6 09	7 04	163.9	58.8	36
25	427	415	371	305	218	121	39	8						6 40	7 37	202.8	68.5	34
Apr 1	506	489	443	376	284	184	88	26	4					7 24	8 28	257.0	83.0	32
5	546	532	487	412	321	219	116	45	11					7 52	8 59	289.6	91.4	31
10	595	583	541	471	380	272	165	78	26	6				8 28	9 46	338.2	101.9	30
15	639	628	588	522	430	326	214	113	50	17	5			9 06	10 57	385.5	112.6	29
20	683	669	630	567	480	374	261	153	77	32	12	5	2	9 52		432.6	123.7	29
25	722	709	671	610	529	422	312	204	114	54	26	14	8	11 02		484.5	134.8	28
May 1	769	754	715	652	570	470	358	255	161	93	53	32	28			542.1	147.1	27
5	800	788	746	682	595	494	391	285	192	124	77	51	43			581.5	154.0	27
10	836	821	782	717	629	532	425	323	231	158	107	76	67			630.8	163.6	26
15	865	850	811	746	622	563	460	358	264	187	133	105	94			674.8	170.4	25
20	893	876	839	774	691	591	491	386	291	215	160	128	118			713.9	176.5	25
25	915	900	860	799	713	618	514	412	319	242	186	150	139			748.5	181.8	24
Jun 1	910	896	859	798	722	625	526	427	339	259	205	169	160			763.3	160.8	21
5	919	907	869	809	731	637	538	440	350	273	218	184	172			780.4	162.8	21
10	918	905	867	806	726	634	535	439	355	281	227	191	180			784.5	136.6	17
15	924	911	873	812	733	638	543	447	360	288	234	198	188			796.0	137.3	17
21	925	913	875	814	736	643	547	451	366	291	236	203	192			798.6	137.3	17
25	923	911	873	812	734	642	545	450	365	290	235	202	190			797.4	137.3	17

Table A.1. (continued)

Hour angle = True solar time − 12h		00	01	02	03	04	05	06	07	08	09	10	11	12	Sun on horison h m	$g_0 = 0$ h m	Daily insolation G_0 ly/day	D ly/day	D/G_0 %
Jul	1	903	894	853	793	714	624	527	431	349	277	224	190	179			769.4	133.3	17
	5	882	868	834	774	694	605	509	415	335	264	212	180	168			745.5	129.0	17
	10	868	855	820	759	680	588	495	401	319	249	197	162	153			723.8	127.0	18
	15	854	840	802	741	665	572	476	382	299	229	178	146	135			698.6	125.2	18
	20	835	822	783	723	645	552	456	363	282	212	161	127	116			671.6	122.2	18
	25	812	797	759	699	621	528	431	340	258	188	136	107	98			638.1	119.8	19
Aug	1	777	764	724	663	583	488	390	300	218	148	102	74	66			584.8	116.5	20
	5	756	742	704	638	560	463	365	274	192	128	82	54	51			552.4	116.0	21
	10	722	706	666	602	520	426	333	239	161	97	54	33	29			505.0	109.0	22
	15	684	669	630	566	487	389	298	207	129	68	33	20	16			461.2	102.1	22
	20	641	628	589	525	444	350	255	168	96	42	19	7	5	10 24		413.5	94.0	23
	25	600	584	544	480	399	309	216	132	61	23	5	1	0	9 30		366.0	85.8	23
Sep	1	540	526	489	420	343	250	158	78	27	7				8 32	9 54	307.5	73.6	24
	5	505	491	450	388	305	216	124	51	17	2				8 06	9 15	275.2	66.1	24
	10	456	442	402	342	259	171	87	30	6					7 31	8 34	235.8	60.1	26
	15	403	390	354	293	213	125	51	13						6 59	7 58	197.3	52.9	27
	20	355	344	301	242	164	85	30	4						6 28	7 24	161.8	46.7	29
	25	301	288	250	190	118	51	12							5 57	7 03	127.5	40.4	32
Oct	1	244	234	194	138	73	25	3							5 23	6 16	94.6	33.4	35
	5	211	197	158	106	48	12								4 56	5 50	75.1	28.4	38
	10	156	143	110	63	25	4								4 24	5 20	50.7	22.3	44
	15	111	102	71	35	11									3 50	4 50	33.0	16.9	51
	20	74	64	42	19	2									3 14	4 15	19.7	12.4	63
	25	44	38	23	7										2 32	3 47	10.6	8.4	79
	30	24	20	9	1										1 36	3 12	4.9	4.6	94
Nov	3	14	8	2											0 00	2 46	2.0	2.0	100
	14	0														0 00	0	0	-

Figure A.2. Curves relating the effect of cloud type and month on the amount of incoming solar radiation received at Truelove Lowland, N.W.T..

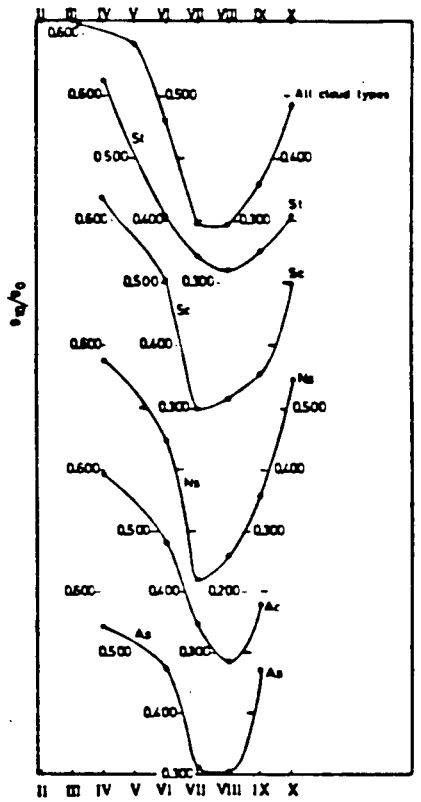
II III IV V VI VII VIII IX X
0.600
0.500
0.400
0.300
0.200
All cloud types
St
Sc
Ns
Ac
As
θ_{ij}/θ_0

2) A program from the IMSL library, IQHSCU, computed the coefficients for a set of cubic polynomials, which were then used by another program from this library, DCSQDU, to interpolate between the hourly data points to calculate half-hourly radiation values.

3) The area between these half-hourly points was then integrated (with DCSQDU) and divided by 30 (min) to calculate the mean half-hour radiation value in $mcal.cm^{-2}.min^{-1}$, resulting in insolation values corresponding to 12^{15},12^{45},13^{15} etc..

4) A program,DCSQDU, was then used to integrate the total area under the curve defined by the half-hour values to compare with Dahlgren's calculated G_0 values. The result of the integration was divided by 1000 (to convert $mcal.cm^{-2}$ to $cal.cm^{-2}$, which is a langley) and multiplied by 2 to arrive at a daily total. The integrated insolation values computed by the above method agreed within 1% of Dahlgren's calculated G_0 values.

5) These mean half-hourly data were then multiplied by 0.0956 to convert the data from $mcal.cm^{-2}.min^{-1}$ to $mE.m^{-2}.min^{-1}$ resulting in Photosynthetically Active Radiation (PAR) data (see Appendix B).

6) The sun was above the horizon continuously from 1 June to 17 August at this location, and the solar altitude from 24^{00} to 12^{00} h is the mirror image of the solar altitude from 12^{00} to 24^{00} h during this time. The shape of each diurnal curve was thus defined by

graphing half-hourly insolation values from 24^{00} to 12^{00} h followed by the same values graphed from 12^{00} to 24^{00} h, assuming an unobstructed horizon.

The result of steps 1 to 6 provided global radiation data for a continuously clear sky from June 1 to August 17, the maximum amount of insolation possible during this time. To estimate insolation under cloudy and overcast sky conditions, two more datasets were computed.

Cloud cover corrected model

Cloud cover observations were made at Cape Vera as part of the twice daily aviation weather reports transmitted to Resolute Bay. These observations consisted of cloud type and the amount of sky covered by each type, and were made by three observers during the summer. They are the only cloud data available for June 1 to August 17 1982, since Landsat and NOAA satellite imagery was unusable for this purpose.

I used Dahlgren's monthly mean relative insolation (g_{10}/g_0) values to calculate the relative insolation from these twice daily (07^{00} and 19^{00}h) cloud observations as follows:

1) The monthly values of g_{10}/g_0 were graphed, manually curve-fitted and a cloud cover correction factor (cccf) recorded for each day from June to August.

2) The total cloud cover (cc) from each field observation was calculated by summing the amount of sky covered by each type of

cloud, for example, 3/10 stratus, 5/10 altocumulus and 1/10 cirrus gave 9/10 total cloud cover.

3) To calculate the daily insolation under 'actual' conditions, G' was calculated for each observation :

$$G' = cc * cccf * G_0 + (1 - cc * G_0)$$

where G'= actual insolation with corresponding cloud cover (langleys/day)

cc= cloud cover (in tenths)

cccf= cloud cover correction factor (step 1)

G_0= daily global radiation with a clear sky

The G'_{0700h} and G'_{1900h} values were averaged for each day.

(Although several equations have been proposed to calculate daily insolation at actual cloudiness, (Vollenweider 1969, Vowinckel and Orvig 1962) most rely on empirical constants untested in the Arctic. The equation used here was suggested by B. Alt (pers.comm.), and was the most suitable for the data available.)

4) A ratio of G'/G_0 was calculated for each day.

5) Each hourly value from Dahlgren's original clear sky insolation dataset (after interpolation between days) was then multiplied by the corresponding daily ratio of G'/G_0.

6) Steps 2 to 7 from the clear sky model were then repeated with this cloud cover corrected dataset. Integration of the area under the daily curves produced the calculated G' value within 1%.

Dahlgren calculated monthly means of relative insolation G/G_0 based on actual cloudiness; his values for June and July (the means of 1961/62) were 0.743 and 0.651 respectively. The modelled mean cloud cover corrected data values of relative insolation at Cape Vera were 0.524 and 0.660 for June and July.

Densely Overcast Model

Insolation was also calculated for a continuous 10/10 cloud cover from June to August using Dahlgren's data to estimate the minimun amount of insolation available. This calculation was the same as that used in the cloud cover model except the following equation was used in step 3:

$$G_{10}=cccf*G_0$$

where G_{10} = insolation with 10/10 cloud cover

cccf = daily cloud cover correction factor

G_0 = daily global radiation with a clear sky

The calculation of G_{10} was done once a day.

The three insolation datasets are presented graphically (Fig. A.3).

Figure A.3. Incoming solar radiation calculated at Cape Vera with cloudless, cloud-cover corrected, and 10/10 overcast sky conditions.

SOLAR RADIATION CLIMATES FOR CAPE VERA, NWT

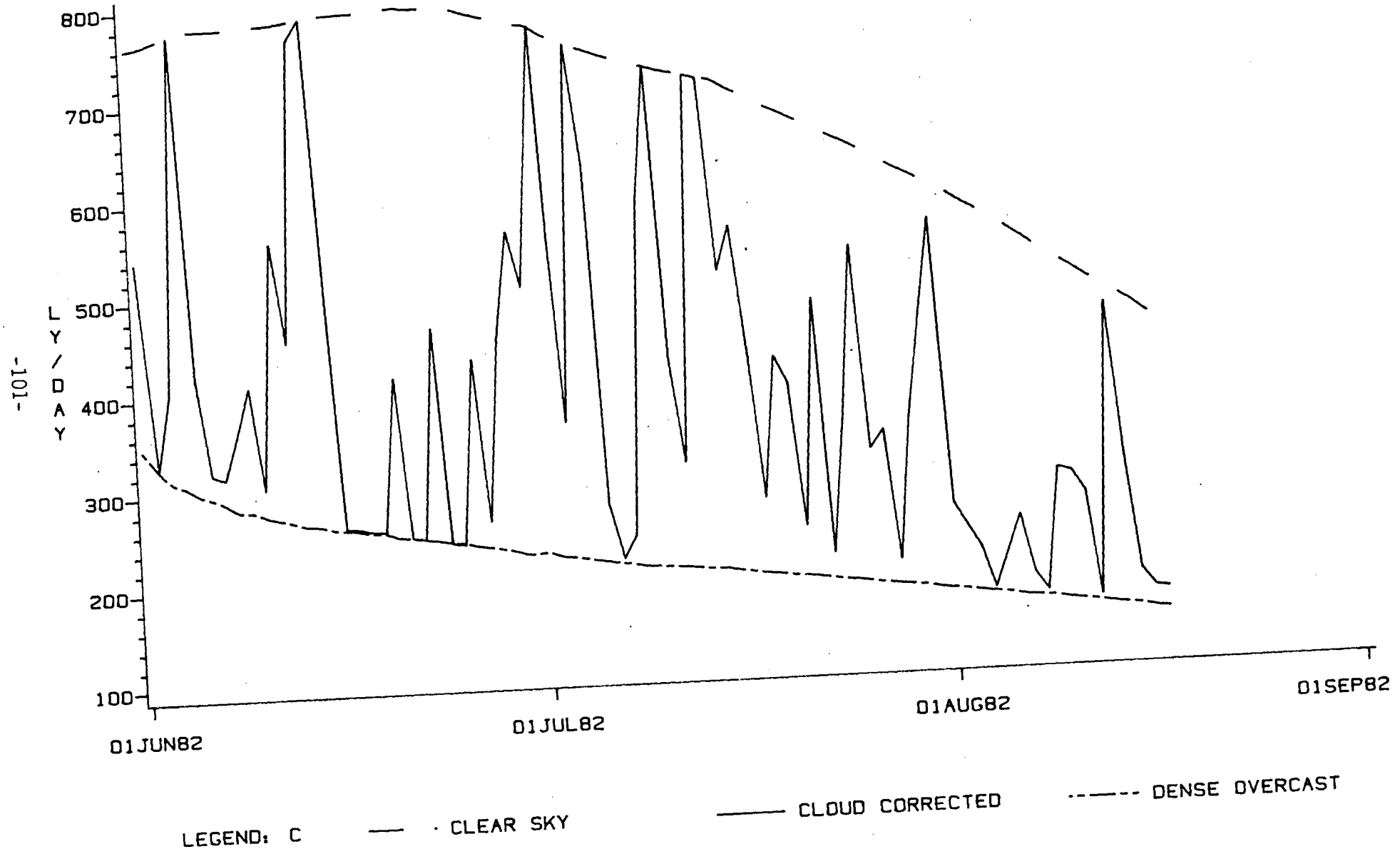

APPENDIX B

CONVERSION FACTORS FOR SOLAR RADIATION MEASUREMENTS

The wavelengths of solar radiant energy reaching the earth's surface range from approximately 290 to 3000 nm, and include near ultraviolet (290-380 nm), 'light', or radiation visible to the human eye (380-760 nm), and infra-red (760-3000 nm) (Luning 1981). Fifty percent of the total energy of this spectral range is from the waveband 400-700 nm (Szeicz 1974).

Irradiance is the radiant flux received by unit area per unit time, and it can be measured in terms of either energy or quanta. Energy measurements are of the total incident energy of the spectral range from ultraviolet to infra-red. Quanta are fundamental units of energy, and the energy content of these units differs with wavelength (or frequency). Quanta in the visible range are called photons. Shorter wavelengths quanta possess more energy than longer wavelengths quanta, although longer wavelengths contain more quanta (Jerlov and Steeman Nielssen 1974). Quanta measurements are of the number of incident quanta of a specified waveband. Since the photobiochemical process is dependant on the number of quanta absorbed and not on their energy level (because one quantum cannot excite more than one molecule regardless of it's energy level), quanta measurements are often used in primary production work.

Units of Measurement

Energy is usually measured in joules sec^{-1} m^{-2} (1 joule sec^{-1}=1 watt), which are SI (Systéme International d'Unités) units, or calories per unit area per unit time which are often used in meteorology. A calorie is the amount of heat necessary to raise the temperature of 1 gram of water from 14.5 to 15.5°C, and the conversion of calories to joules is the factor 4.184, which is the specific heat of water at 15°C (LeGrand, 1968). Quanta are measured in Einsteins (E), where 1 Einstein is $6.02*10^{23}$ quanta (Avogadro's number).

Conversion Factors

Because measurements of quanta are most appropriate for primary production work, and the light for the C^{14} incubation experiments was measured in uE m^{-2} sec^{-1}, Dahlgren's solar radiation data (in mcal cm^{-2} min^{-1}) had to be converted to quanta units. I assumed that 50% of the total energy Dahlgren measured was photosynthetically active radiation (PAR), and used 4.184 to convert calories to joules.

Energy

1 $cal.cm^{-2}$=1 langley (ly)

1 $ly.sec^{-1}$=4.184 $joules.sec^{-1}.cm^{-2}$ = 4.184 $watts.cm^{-2}$

1 $ly.min^{-1}$=4.184 $joules.min^{-1}.cm^{-2}$

=(4.184/60)$joules.sec^{-1}.cm^{-2}$

=$6.973*10^{-2}$ $watts.cm^{-2}$ ($6.937*10^{2}$ $watts.m^{-2}$)

=693.7 $watts.m^{-2}$

Energy to Quanta

$$1 \text{ watt.m}^{-2} = 4.57 \text{ uE.m}^{-2}.\text{s}^{-1}$$

$$1 \text{ ly.min}^{-1} = 693.7 \text{ watts.m}^{-2} * 4.57 \text{ uE.m}^{-2}.\text{s}^{-1}$$

$$= 3187 \text{ uE.m}^{-2}.\text{s}^{-1}$$

$$1 \text{ mcal.cm}^{-2} \text{ min}^{-1} = 3.187 \text{ uE.m}^{-2}.\text{s}^{-1}$$

Dahlgren's data to Quanta for Solar Radiation models

$3.187 \text{ uE.m}^{-2}.\text{s}^{-1}/\text{mcal.cm}^{-2}.\text{min}^{-1} * 60 \text{ sec/min}^{-1} * 1 \text{ mE}/1000 \text{ uE}$

$*0.5 \text{ (PAR)} = 0.0956 \text{ mE.m}^{-2}.\text{min}^{-1}/\text{mcal.cm}^{-2}.\text{min}^{-1}$